Quaternary Science Advances 6 (2022) 100050

Contents lists available at ScienceDirect

Quaternary Science Advances

journal homepage: www.sciencedirect.com/journal/quaternary-science-advances

# Summer temperatures and environmental dynamics during the Middle Würmian (MIS 3) in the Eastern Alps: Multi-proxy records from the Unterangerberg palaeolake, Austria

Elena A. Ilyashuk [a,*], Boris P. Ilyashuk [a], Oliver Heiri [b], Christoph Spötl [c]

[a] Department of Ecology, University of Innsbruck, Technikerstrasse 25, 6020, Innsbruck, Austria
[b] Geoecology, Department of Environmental Sciences, University of Basel, Klingelbergstrasse 27, CH-4056, Basel, Switzerland
[c] Institute of Geology, University of Innsbruck, Innrain 52, 6020, Innsbruck, Austria

ARTICLE INFO

*Keywords:*
Palaeotemperature
Marine isotope stage 3
Chironomids
Carbon and oxygen isotopes
Charophytes

ABSTRACT

Several millennial-scale warm phases perturbed the glacial climate during Marine Isotope Stage 3 (MIS 3, ca. 57–29 ka BP). Little is known about the impact of these climatic changes on Alpine ecosystems due to the sparsity of undisturbed sediment records in the Alps and their foreland. In this study, multiple sediment-archived proxies (sediment geochemistry, stable oxygen and carbon isotopes of autochthonous carbonate, and subfossil remains of macrophytes and aquatic invertebrates) were examined in five drill cores from an ancient inner-Alpine lake at Unterangerberg (Eastern Alps) to reconstruct the palaeolake environment and to estimate summer temperature changes for the first half of MIS 3. The lacustrine sedimentation in the basin began ca. 54.6 ka, tentatively correlated with the start of Greenland Interstadial (GI) 14. We identified three distinct phases in the development of the lake. (1) A cold, oligotrophic water body influenced by snow/glacier meltwater ca. 54.6–52.2 cal ka BP. (2) A clear-water, macrophyte-dominated, productive lake ca. 52.2–44.9 cal ka BP. Submerged macrophytes were dominated by the charophyte alga *Chara hispida* and chironomid assemblages – by *Corynocera ambigua*, which is absent from the present-day fauna of the Alpine region. (3) A turbid-water, less productive lake ca. 44.9–41.5 cal ka BP. This shift towards a turbid-water state, as evidenced by the drastic reduction in the abundance of submerged macrophytes and associated invertebrates, likely occurred due to increased input of meltwater. The regime shift is tentatively correlated with the start of GI 11, for which the highest temperatures of the studied MIS 3 interval are inferred. Chironomid-based reconstructions of mean July air temperatures provide interstadial temperature estimates between ca. 11 and 12.5°C (i.e. ca. 5–6°C below present-day values), which concurs with reconstructions available from the northern Alpine foreland. Cooler July temperatures (ca. 9–10°C) are reconstructed for MIS 3 stadials. The Unterangerberg lacustrine records provide valuable new insights into MIS 3 climate dynamics inside the Eastern Alps and contribute to a better understanding of the effects of climate change on the Alpine environment.

## 1. Introduction

Large variations in climate that occurred in the North Atlantic realm during the last glacial period are well documented in Greenland ice cores (Dansgaard et al., 1993; Wolff et al., 2010) and deep-sea sediments (Shackleton et al., 2000). In particular, Marine Isotope Stage 3 (MIS 3, ca. 57–29 ka BP; Lisiecki and Raymo, 2005), also known as Middle Würmian in the Alpine Quaternary stratigraphy (Preusser, 2004; Heiri et al., 2014), was characterised by great climate instability resulting from abrupt changes between stadial and interstadial conditions. Several large-amplitude millennial-scale cycles of rapid warming and gradual cooling, so-called Dansgaard-Oeschger (DO) cycles, have been described in Greenland ice cores for MIS 3 (Rasmussen et al., 2014; Li and Born, 2019). This stage, being sandwiched between periods of sea-level lowstands (MIS 4 and MIS 2), was a time of intermediate global ice volume, when global sea level ranged between 60 and 90 m below present, with a higher stand during the first half of MIS 3 (Siddall et al., 2003, 2008). Aridity reconstructions for the last 60 ka in eight key regions of the global climate system show that central Europe was humid during early MIS 3, intermediate conditions prevailed during mid-MIS 3,

* Corresponding author.
*E-mail address:* eilyashuk52@gmail.com (E.A. Ilyashuk).

https://doi.org/10.1016/j.qsa.2022.100050
Received 22 November 2021; Received in revised form 27 December 2021; Accepted 4 January 2022
Available online 6 January 2022

and an arid period occurred at the end of MIS 3 (Fuhrmann et al., 2020).

The European Alps were probably characterised by a highly variable glacier extent during MIS 3 (cf. Seguinot et al., 2018) but little direct evidence is available given the pervasive MIS 2 advance. Speleothems, as climate archives providing a superior chronology, have been particularly valuable in characterising regional MIS 3 climate variability on millennial and shorter timescales. Stable oxygen isotope records from caves on the northern rim and in the central Alps provide precise constraints on the timing and duration of major climatic events and revealed a pattern strongly resembling that of Greenland ice cores (Spötl and Mangini, 2002; Holzkämper et al., 2005; Spötl et al., 2006; Moseley et al., 2014). Unfortunately, however, speleothems lack a direct proxy for land surface conditions and ecosystem changes.

Investigations of cave systems in the Eastern Alps suggest that even during major interstadials of MIS 3 glaciers were significantly larger than throughout the Little Ice Age (ca. AD 1300–1850) (Spötl and Mangini, 2007). Yet, major inner-Alpine valleys remained ice-free at least during the first half the MIS 3, as evidenced e.g. by radiocarbon data of mammoth fossils (Spötl et al., 2018). The existence of lakes/ponds in unglaciated and vegetated catchments within MIS 3 is recorded in some inner-Alpine sites, such as Unterangerberg (Starnberger et al., 2013a) and Baumkirchen (Barrett et al., 2017) in the Inn valley, and Nesseltalgraben in Berchtesgaden (Mayr et al., 2017, 2019; Stojakowits et al., 2020). However, MIS 3 lacustrine successions are not widespread in the Alps and their northern foreland because of the subsequent ice advance and associated glacial erosion during MIS 2. Only a few lacustrine records of Middle Würmian age have been studied in Alpine sites in Switzerland, Austria and Germany (Heiri et al., 2014). Pollen, as a proxy for past vegetation, have been mainly used for inferring stadial/interstadial conditions from these archives and examining the impact of rapid climate changes on terrestrial ecosystems. The effects of these climatic events on freshwater habitats, however, remain poorly known.

Subfossil assemblages of aquatic biota (algae, macrophytes, and invertebrates) preserved in lacustrine sediments are also important proxies for palaeoclimate, which provide direct information on in-lake processes and contribute to understanding the diversity of lake responses to changes in climate (Cumming et al., 2012). Chironomids (non-biting midges; Insecta: Diptera: Chironomidae), generally the most abundant and diverse macroinvertebrates found in freshwater ecosystems, have received attention by researchers worldwide due to the robustness of their response to changes in environmental variables (Ferrington, 2008; Walker, 2013). Of the organism groups preserved as subfossils in lake sediments, chironomids are presently one of the few palaeoclimatic indicators which, with the aid of numerical chironomid-based inference models, can provide quantitative estimates of past temperature changes (Brooks, 2006; Eggermont and Heiri, 2012). Still, chironomid-based studies on lacustrine sediments dating back to MIS 3 from Europe are scarce. To our knowledge, only a few studies focused on chironomids in the MIS 3 deposits in Finland (Helmens et al., 2007, 2018; Engels et al., 2008a, 2014; Helmens and Engels, 2010) and Germany (Becker et al., 2006; Engels et al., 2008b, 2008c; Bolland et al., 2021a). This is probably due to the generally dry and compact nature of glacial deposits, low fossil content and often poor preservation of the remains, making the analysis particularly time-consuming (e.g. Engels et al., 2008c; Bolland et al., 2021a, 2021b).

Only few proxy datasets have been used for quantifying past temperature during MIS 3 in the Alpine region. Studies based on fossil beetle assemblages from Gossau and Niederweningen (Jost-Stauffer et al., 2005; Coope, 2007), and stable isotope data of mammoth teeth from Niederweningen (Tütken et al., 2007), sites in Switzerland, suggest that Middle Würmian interstadial summer and annual temperatures in the Swiss northern Alpine foreland were around 4–6°C lower than today. Chironomid assemblages at Füramoos in the northern foreland of the Eastern Alps (southern Germany) indicate mean July temperatures up to 6°C lower than present (Bolland et al., 2021a). To our knowledge, quantitative temperature estimates from the Eastern Alps are lacking for this time interval.

Here, we present chironomid records, along with other aquatic bioindicators (non-chironomid invertebrates, macrophytes) and abiotic proxies (sediment geochemistry, stable oxygen and carbon isotopes of lacustrine carbonates), derived from a palaeolake that existed at Unterangerberg (western Austria) during the first half of MIS 3. Previous research of this site focused on field evidence, lithological description of drill cores, age determination using radiocarbon and luminescence, sedimentological and palynological investigations (Starnberger et al., 2013a, 2013b) as well as on the multi-proxy reconstruction of climate conditions for the Early Würmian (MIS 5a) (Ilyashuk et al., 2020). This study aims to reconstruct the environmental history of the paleolake and to provide insights into processes and causes of the lake ecosystem responses to climate variability, as well as to estimate summer temperature changes inferred from chironomid assemblages for the studied MIS 3 interval.

## 2. Study site and analysed sediment sections

Valley terraces are a characteristic morphological element of the central and lower Inn valley. The study site, the inner-Alpine valley terrace of Unterangerberg (47°30′ N, 12°00′ E; 630 m a.s.l.; ca. 34 km$^2$) is situated ca. 1 km northwest of the city of Wörgl (Fig. 1), bounded by the Inn River in the southeast and surrounded by mountain ranges with altitudes of up to 1637 m a.s.l. to the north and northwest. The terrace lies approximately 100–150 m above the valley floor. The base of the terrace is formed by partly lithified fluvial sediments of the Upper Oligocene Angerberg Formation (Ortner and Stingl, 2001). At the meteorological station at Kufstein (492 m a.s.l.) ca. 8 km downstream of the terrace, the mean July air temperature is 18.2°C for the most recent climate normal period 1981–2010 (data source: Central Institute for Meteorology and Geodynamics, Austria; https://www.zamg.ac.at/cms/de/klima/klimauebersichten). Taking into account the lapse rate of 0.65°C per 100 m in the Alps (Böhm et al., 2001), the mean July air temperature calculated for the altitude of the Unterangerberg terrace is 17.3°C.

Geophysical exploration and numerous drillings in 1995–2006 revealed a SW–NE striking depression filled by up to 150 m of Pleistocene sediments. The lithostratigraphy of seventeen drill cores with lengths between ca. 40 m and 200 m studied by Starnberger et al. (2013a) varies greatly from core to core, highlighting the complex depositional pattern in the subsurface of the terrace. The Upper Pleistocene sedimentary succession comprises diamict, gravel, sand, lignite and thick intervals of fine grained sediments.

The youngest and best preserved lake phase was identified in five cores (Fig. 2), A-KB 13/98 (26–28 m depth), A-KB 14/98 (44–49 m depth), A-KB 15/98 (16–22 m depth), A-KB 16/98 (31–38 m depth) and A-KB 17/98 (29–34 m depth), recovered from the terrace during a drilling campaign in 1998. A detailed description of the cores is given in Starnberger et al. (2013a). Radiocarbon and optically stimulated luminescence (OSL) dating indicate the existence of a palaeolake between ca. 55 and 40 ka BP (Starnberger et al., 2013a, 2013b). In this study the lacustrine sections consisting of fine sand and organic-rich silt from all five cores were analysed.

## 3. Methods

### 3.1. Sediment sampling

The 6-m lacustrine section of core A-KB 15/98 obtained from the deepest area of the palaeolake (Fig. 2) was sampled every ca. 20–30 cm for geochemical and chironomid analyses. In total 24 samples were taken from the core. Additionally, 10 samples at 30–50 cm intervals were obtained from core A-KB 17/98 that originates from the shallow-water area of the palaeolake and is exceptionally rich in fossils. Seven,

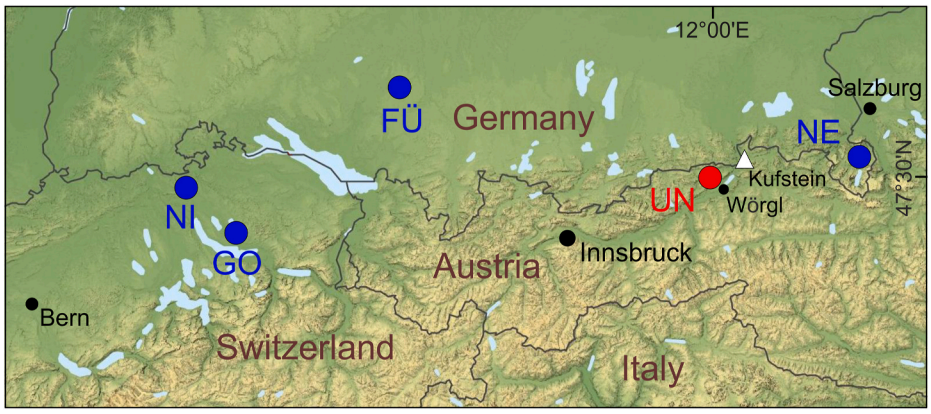


**Fig. 1.** Map showing the location of the Unterangerberg (UN) site in the northern Alps and other sites mentioned in the text: GO – Gossau, Fü – Füramoos, NE – Nesseltalgraben, NI – Niederweningen. The white solid triangle represents the weather station at Kufstein. The map was produced using stepmap (www.stepmap.com).

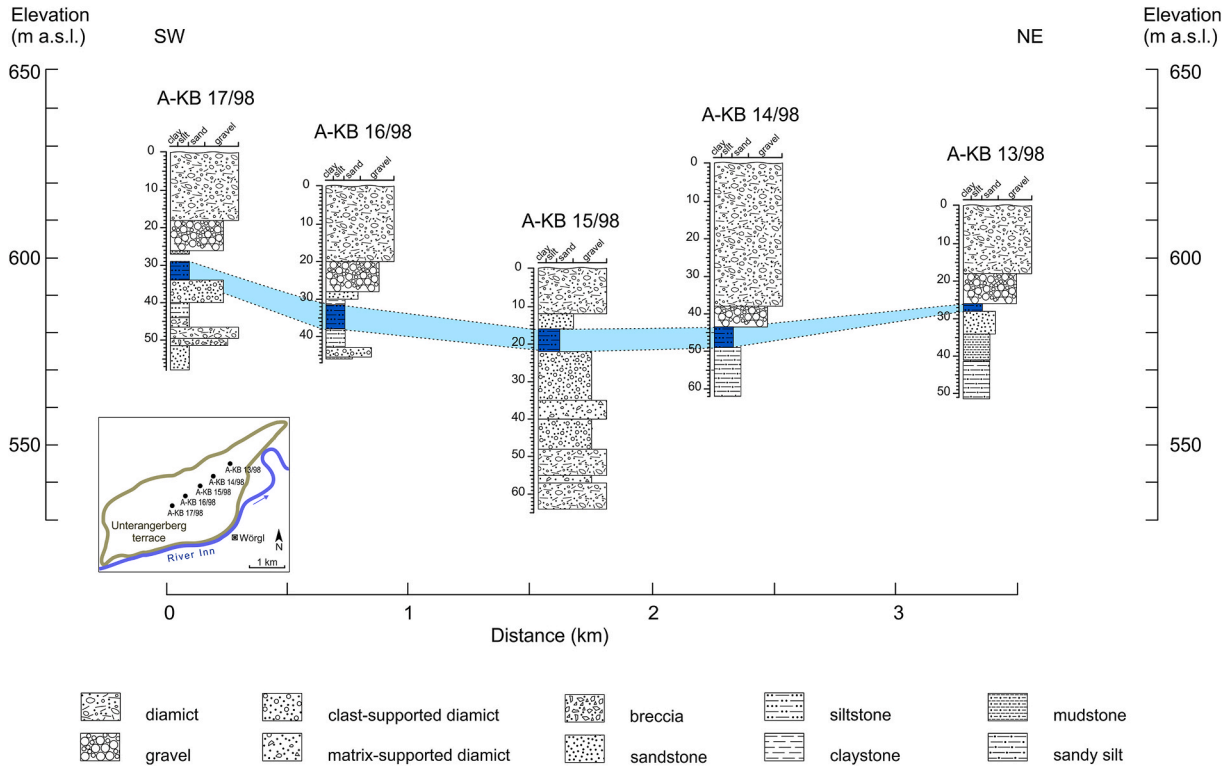


**Fig. 2.** The Unterangerberg terrace with the locations of the drill sites (solid circles) along a SW–NE profile, schematic view and main sedimentary characteristics of the cores; lacustrine sediments are highlighted in light blue (modified after Starnberger et al., 2013a). (For interpretation of the references to colour in this figure legend, the reader is referred to the Web version of this article.)

four and three samples were also analysed from cores A-KB 16/98, A-KB 13/98 and A-KB 14/98, respectively.

### 3.2. Additional radiocarbon dating and age-depth model

For the MIS 3 lacustrine section in core A-KB 15/98, obtained from the deepest area of the palaeolake, two OSL dates on quartz and polymineral fine-grain fractions of 44 ± 4 and 55 ± 5 ka BP were obtained at 17.4 and 21.7 m depths, respectively (Starnberger et al., 2013a). We supplemented the chronological control for the section by the accelerator mass spectrometry (AMS) radiocarbon date of 39.4 ± 1 $^{14}$C ka BP (Lab. no. Poz-96477; 43.3 ± 1.2 cal ka BP) derived from a wood twig found at 16.9 m depth. The calibration of the radiocarbon date and modeling of the age-depth relationship was performed using OxCal 4.4.2 (Bronk Ramsey, 2009) that uses the IntCal20 dataset (Reimer et al., 2020). The OSL and $^{14}$C ages, which are all in stratigraphic order, were used to develop a Bayesian age-depth model that was constructed using the P_Sequence (Poisson mediated deposition) procedure with the parameter *k* of 100 (Bronk Ramsey, 2008), and linear interpolation between the median probability ages (Fig. 3).

### 3.3. Sediment geochemistry and stable isotopes

Total carbon (TC) and total nitrogen (TN) were measured with a Carlo Erba Flash 1112 series elemental analyser (ISO 10694, 1995 and ISO 13878, 1998). Total inorganic carbon (TIC) was analysed with the

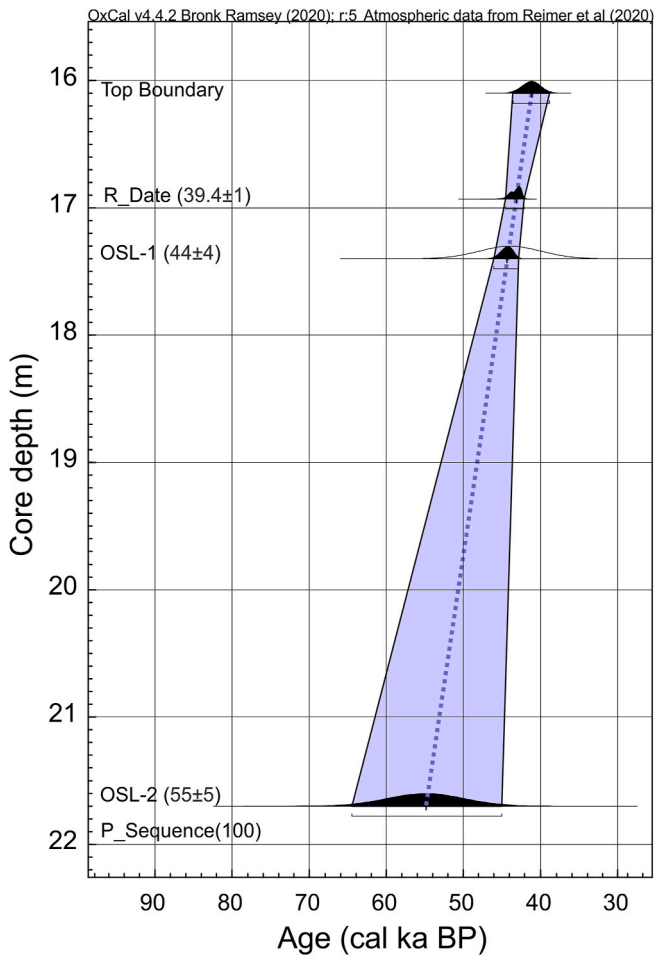


**Fig. 3.** OxCal age-depth model for the record of core A-KB 15/98 using radiocarbon and OSL dates. The shaded area indicates the fitted model with the 95% confidence ranges and the stippled line indicates the median age-depth model.

same method and device after pre-combustion in a furnace at 500°C for 2 h to remove the organic fraction. TN, TC and TIC are expressed in weight percentage (wt%) of the sediment. Total organic carbon (TOC), a primary proxy for the organic matter content of lake sediments, was calculated by subtracting TIC from TC. The C/N ratio was calculated as the element mole TOC/TN ratio. The TIC content was converted to calcium carbonate ($CaCO_3$) by multiplying with a factor of 8.33 based on the molar mass of carbon relative to $CaCO_3$. The amount of organic and inorganic matter (OM and IM) was determined by loss on ignition at 550 °C following Heiri et al. (2001). The $CaCO_3$ data are represented as weight percentage of the IM fraction (im%). All these parameters were measured and calculated for the same sediment samples where also the chironomid were analysed.

Stable oxygen ($\delta^{18}O$) and carbon ($\delta^{13}C$) isotope values were obtained on calcite originating from encrustations of charophytes (Charales) formed in summer, calcite 'stem-tubes' and walls of gyrogonites (calcified oospores). Samples of disintegrated calcite encrustations (200–300 μg) were collected under a stereomicroscope at 10–30 × magnification with tweezers from the residue left after washing aliquots of sediment samples through a 200 μm sieve (Hammarlund et al., 1999, 2003). The isotopic composition of 12 calcite samples from cores A-KB 17/98 and A-KB 13/98 obtained from shallow-water areas of the palaeolake, where calcite encrustations are abundant, was determined using a Thermo Scientific Delta V Plus continuous-flow mass spectrometer linked to a GasBench II. Calibration of the instrument was accomplished using international calcite standards (NBS18, NBS19, CO1, CO8) and the results are reported in permill (‰) notation on the Vienna Pee Dee Belemnite (VPDB) scale. Further analytical details can be found in Spötl and Vennemann (2003).

### 3.4. Chironomid analysis

Sediment samples for chironomid analysis were processed following Walker (2013) with additional ultrasonic treatment to disintegrate the densely compacted sediments. The preparation included chemical pre-treatment with warm 10% KOH for 1 h, subsequent rinsing through a 100 μm sieve, treatment of the residues in an ultrasonic bath (40 kHz) for 5 s, and another follow-up rinsing through a 100 μm sieve. Chironomid larval head capsules (HC) were then hand-picked from the sieve residue in a Bogorov tray under 20–40 × magnification, dehydrated in 100% ethanol and permanently mounted ventral side up on microscope slides in Euparal® mounting medium for taxonomic identification. Head capsules were identified under 200–400 × magnification with keys for larvae (Brooks et al., 2007; Andersen et al., 2013). At least 50 chironomid head capsules, a representative number for quantitative inferences, were counted and identified in each sample (Heiri and Lotter, 2001). Depending on the chironomid abundance, about 3–20 g of dry sediment were processed for organic-rich silty layers and 100–200 g for organic-poor layers. Head capsule concentrations are based on numbers per gram of dry sediment (HC/g DW). Zonation of the chironomid stratigraphies was done using the technique of optimal splitting by information content and the number of statistically significant zones was identified with the broken stick model (Bennett, 1996) using the Psimpoll 4.27 software (Bennett, 2009).

### 3.5. Macrophytes and non-chironomid invertebrates

During the sorting chironomid subfossils, remains of non-chironomid aquatic invertebrates such as exoskeletons of oribatid mites (Acarina: Oribatida), shells of molluscs (Mollusca: Gastropoda, Bivalvia), and mandibles of caddisflies (Insecta: Trichoptera) and the alderfly *Sialis* (Insecta: Megaloptera) as well as macro-remains of mosses and charophyte fructifications (oospores and gyrogonites) were picked and identified. Species identifications of mosses followed the key of Van de Weyer and Schmidt (2018a, 2018b). The key of Haas (1994) was used to identify charophyte fructifications. The number of macrofossils (NbM) of plants and non-chironomid invertebrates were counted for 50 g of dry sediment.

### 3.6. Chironomid-based temperature reconstruction

Mean July air temperatures were reconstructed using a combined Swiss-Norwegian chironomid–temperature inference model described by Heiri et al. (2011). This model includes information on the distribution of 154 chironomid taxa in 274 lakes in temperate, subarctic, arctic, and Alpine environments over a July air temperature range of 3.5–18.4°C. The combined data-set covers a larger temperature range than most other existing regional calibration data-sets. The transfer function was developed using weighted averaging partial least squares (WA-PLS) regression (ter Braak and Juggins, 1993) with two components and yielded a bootstrapped coefficient of determination between inferred and observed July air temperature values of 0.87 and a root mean square error of prediction of 1.4°C. The inverse regression approach assumes an explicit unimodal underlying taxon–environment response model, involves global estimation of environmental optima for taxa, and is statistically robust (Birks et al., 2010). The method is appropriate for estimating past temperatures even if fossil assemblages do not have close analogues in the modern environment, as long as the individual taxa are well represented in the modern calibration data (Lotter et al., 1999).

To evaluate the performance of the model we applied several criteria. Sample-specific errors as a quantitative estimate of the

uncertainty in the reconstructed values (Juggins and Birks, 2012) were estimated using bootstrapping (9999 iterations). An evaluation of modern analogues for each sample was performed using the modern analogue technique (Birks et al., 1990) with squared chi-square distance as a dissimilarity measure. The cut-level of the 5th percentile of all distances in the modern data was taken to define samples with 'no good' analogues in the calibration data. Goodness-of-fit to temperature of the down-core assemblages was tested by passively positioning the down-core samples in a canonical correspondence analysis (CCA) of training set samples with July air temperature as the only constraining parameter. Any down-core samples with a squared residual distance to the first CCA axis larger than the 90th and 95th percentiles of the residual distances of all the modern samples were identified as having a 'poor' fit or 'very poor' fit with temperature, respectively (Birks et al., 1990).

## 4. Results and interpretations

### 4.1. Chironomid records and geochemical proxies

In total, 48 chironomid taxa were identified in the Unterangerberg MIS 3 palaeolake. Of these, 13 taxa have relative abundances lower than 2%. Counts of identifiable HC range from 45 to 178 (mean = 104) per sample. All taxa except *Corynocera ambigua* are currently known from the European Alps.

#### 4.1.1. Notes on Corynocera ambigua

In the Alpine region, *C. ambigua* was found in late-glacial and early Holocene lake sediments (Larocque-Tobler et al., 2010) but is absent in modern chironomid assemblages as indicated by analyses of chironomid remains in surface lake sediments (Heiri et al., 2011). Its present distribution is restricted to arctic and subarctic regions, where it lives in small/medium-sized lakes of shallow/moderate depth with oligo-mesotrophic waters and low rates of nutrient input. Temperature optima of this taxon in various calibration data-sets from northern parts Europe, Asia and North America vary between 6°C and 14°C (Larocque et al., 2001; Barley et al., 2006; Luoto, 2009; Porinchu et al., 2009; Heiri et al., 2011; Self et al., 2011). *C. ambigua* larvae can be common in warm-temperate lakes as well (Brodersen and Lindegaard, 1999; Porinchu and Cwynar, 2000; Medeiros and Quinlan, 2011), possibly surviving the high summer temperatures as eggs in the lake sediments and having a growth period over autumn and winter (Mothes, 1968). The development and expansion of *C. ambigua* is facilitated in clear waters favourable for an abundant cover of calcium-fixing macrophytes such as charophytes (Brodersen and Lindegaard, 1999). Shortly after deglaciation of many areas where limestones and other calcareous rocks occur, the chemical composition of water and sediments in lakes was mainly determined by the local geology, namely carbonate-rich till and carbonate bedrock. Accordingly, *C. ambigua* and charophytes are often dominant components in pioneer assemblages of lakes formed after glacier retreat (e.g. Heiri and Millet, 2005; Ilyashuk et al., 2005, 2013; Gandouin et al., 2016).

#### 4.1.2. Core A-KB 15/98, the deepest area of the palaeolake

The lacustrine sediments in core A-KB 15/98 originated in the deeper water of the palaeolake (Fig. 2), where sedimentation of fine material occurs, and assemblages are assumed to consist of a homogenized mixture of biota from different habitats. The section was split into three statistically significant chironomid assemblage zones (Fig. 4).

Zone U15–C-1 (21.6–20.6 m depth) is characterised by high abundances of *Micropsectra radialis*-type (25–39%), *Tanytarsus lugens*-type (7–30%) and *Paracladopelma* (5–17%), which are typical of cold environments (Lotter et al., 1997; Heiri et al., 2011). In lowland lakes *T. lugens*-type and *Paracladopelma* typically occur in the hypolimnion of deep stratified lakes (Heiri and Lotter, 2008). Other cold-adapted taxa *Paracladius*, *Stictochironomus rosenschoeldi*-type and *Paratanytarsus austriacus*-type (Heiri and Lotter, 2010) are present at low abundances. The high abundance of *Chironomus anthracinus*-type (up to 37%) and *Procladius* (up to 20%), which are tolerant of hypoxic conditions (Quinlan et al., 1998) and often form dense populations in deeper parts of lakes, might reflect winter oxygen depletion at the sediment–water interface, possibly as a result of prolonged periods of seasonal ice cover. *Chironomus* is often an early coloniser after significant environmental change where it may live under suboptimal conditions (Brooks et al., 2007). The sediments are characterised by $CaCO_3$ content of ca. 23 im% as well as extremely low values of TOC (<0.5 wt%) and overall low chironomid concentrations (3–4 HC/g DW). Altogether this suggests a relatively cold and oligotrophic lake. The C/N ratio increases towards the end of the

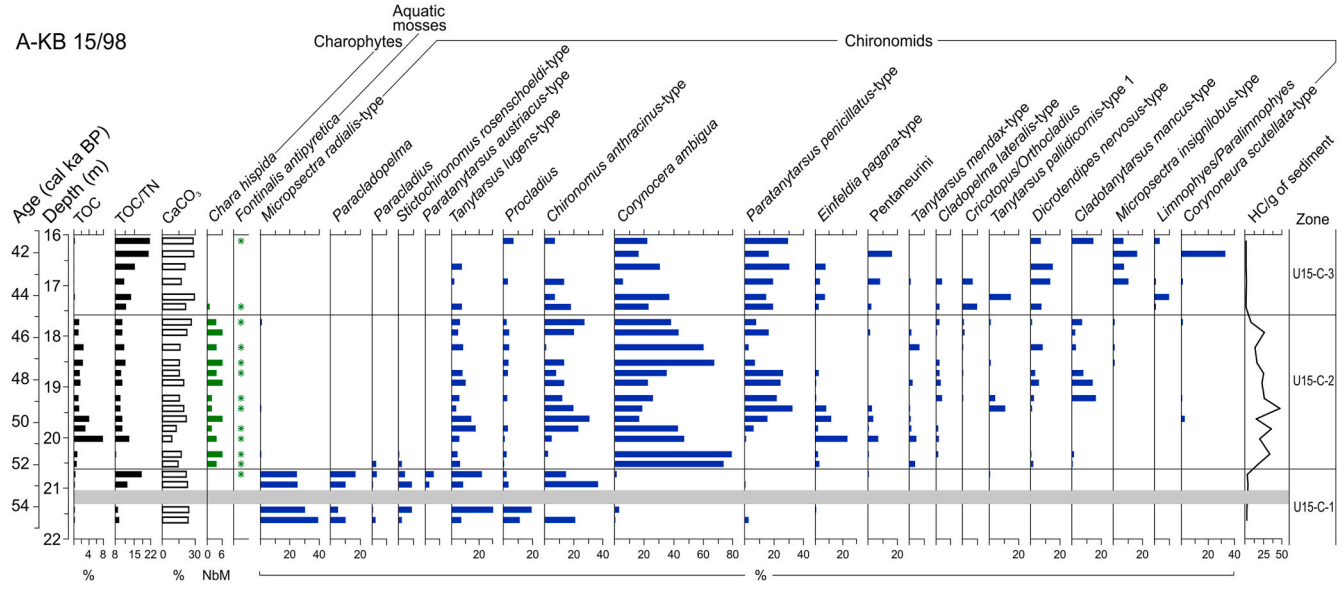


**Fig. 4.** Stratigraphy of the MIS 3 lacustrine deposits in core A-KB 15/98. Percentage values of total organic carbon (TOC), total organic carbon/total nitrogen (TOC/TN) ratios, percentage values of calcium carbonate ($CaCO_3$) in the inorganic fraction, abundance of chironomid head capsules (HC) and charophyte subfossils (NbM = number in 50 g of dry sediment), presence (*) of aquatic moss macrofossils, and relative abundance of the most common (>2%) chironomid taxa arranged from bottom left to top right according to the position of their highest downcore relative frequency. Grey band marks an interval lacking subfossils of aquatic organisms.

zone up to 18, suggesting an increase in terrestrial organic matter input (c.f. Meyers and Teranes, 2001). There is, however, an interval at 21.1–21.4 m depth where no chironomid head capsules and other aquatic invertebrate fossils were found. The sediment properties of this interval (fine-grained sand with clay, almost no TOC and TN) indicate an interruption of the lacustrine sedimentation most likely due to strong cooling and a local glacier advance.

Zone U15–C-2 (20.6–17.5 m depth) is marked by an abrupt shift in chironomid assemblages toward the dominance of *C. ambigua* (17–79%), a species common in oligo-to mesotrophic clear-water lakes. All cold stenotherms recorded in the first zone, except *T. lugens*-type, disappear or become rare. *Paratanytarsus penicillatus*-type (up to 33%), which is indicative of macrophyte-dominated conditions (Langdon et al., 2010; Cao et al., 2014), and *C. anthracinus*-type (up to 32%), which is associated with milder ambient temperatures and elevated organic content of sediments, become co-dominant taxa. Other taxa present in small to moderate numbers, such as *Eintfeldia pagana*-type, *Cladotanytarsus mancus*-type, *Tanytarsus mendax*-type, *Tanytarsus pallidicornis*-type 1, *Dicrotendipes nervosus*-type, and *Cladopelma lateralis*-type, also commonly occur under warmer, more nutrient-rich conditions and/or can be associated with aquatic macrophytes. The chironomid concentration rises in the zone, ranging from 8 to 48 HC/g DW. The changes in chironomid assemblage structure suggest a response to changes in temperature and lake productivity. This is reflected by a distinct increase in the TOC content of the sediment (1–8 wt%). Submerged vegetation is represented by the charophyte alga *Chara hispida* and the aquatic moss *Fontinalis antipyretica.* $CaCO_3$ contents vary between 9 and 26 im%. The C/N ratio falls in the range of 8–13, implying predominantly autochthonous sources, including macrophytes, of the organic matter (Thompson et al., 2018).

Zone U15–C-3 (17.5–16.1 m depth) is generally dominanted by *P. penicillatus*-type (15–31%). *C. ambigua* declines initially (to 6%) but then becomes dominant towards the top of the zone (17–31%). Most notable in the zone is the presence of a mixed assemblage of taxa adapted to cooler, oligotrophic conditions and taxa usually associated with warmer and more fertile environments. The relatively high abundance of *P. penicillatus*-type and other warm-adapted taxa, *C. anthracinus*-type (up to 18%) and *D. nervosus*-type (up to 15%), suggests warmer conditions. *Micropsectra insignilobus*-type, typical of cool well-oxygenated oligotrophic environments, representative of lakes at intermediate altitudes in the Swiss Alps (Heiri et al., 2011), shows a substantial increase (up to 17%) in relative abundance within this zone. The cold-adapted *T. lugens*-type, having a relatively high oxygen demand as well, still persists (2–8%) in the early part of the zone. Chironomids commonly associated with littoral habitats, such as *E. pagana*-type, Pentaneurini, *Corynoneura scutellata*-type, *D. nervosus*-type, *C. mancus*-type, *T. pallidicornis*-type 1 and *C. lateralis*-type, continue to survive, perhaps in suboptimal conditions, and show an episodic presence. Many of these taxa, however, disappear by the top of this zone. The submerged macrophytes *C. hispida* and *F. antipyretica* also vanished in this zone, most likely due to an increase in turbidity and reduced light penetration through the water column. The zone displays very low TOC values (<0.5 wt%) and the chironomid concentration, generally comparable to values in zone U15–C-1, and suggests an overall low lake productivity. The C/N ratio increases up to 21 towards the top of the zone and indicates decreasing input of lake-derived organic matter into the sediments while allochthonous input increased.

#### 4.1.3. Cores A-KB 17/98 and A-KB 16/98, the southwest locations

Sediments of core A-KB 17/98 formed in the littoral zone (Fig. 2) and are exceptionally rich in macrophyte and aquatic invertebrate subfossils (Fig. 5). The section is marked by an overall lower TOC content (≤1.0 wt %) compared to the deep-water sediments (1–8 wt%) deposited during the most productive lake phase (core A-KB 15/98, zone U15–C-2). This indicates a higher organic matter mineralization in littoral rather than in profundal sediments, as commonly observed in temperate shallow lakes where warmer waters in wide littoral areas allow a higher benthic microbial activity during summer (den Heyer and Kalff, 1998). The C/N ratio of 14–17 suggests major contributions of macrophytes to the organic matter of the sediments. $CaCO_3$ contents range from 22 to 28 im %, except for one sample (11 im%) at 30.8 m depth. The chironomid stratigraphy of this section was partitioned into two statistically significant zones (Fig. 5).

Zone U17–C-1 (33.8–32.5 m depth) is characterised by the maximum abundance in each sample of taxa typical of cold environments, including *S. rosenschoeldi*-type (50%), *Paracladopelma* (30%) and *T. lugens*-type (16%), like the initial assemblage from the deep-water sediments (core A-KB 15/98, zone U15–C-1). The exception is the genus *Micropsectra*, which is presented here by *M. insignilobus*-type (with the maximum abundance of 53–79%) associated with cool temperate water in Swiss lakes of intermediate elevation, while in the deep-water sediments the cold-stenothermic *M. radialis*-type, typical of colder and higher elevation lakes, is found (Heiri et al., 2011). *C. anthracinus*-type and *Procladius* are also present. Submerged vegetation is represented by the aquatic moss *F. antipyretica*. Other aquatic invertebrates occur sporadically at low abundance.

In the first half of zone U17–C-2 (32.5–31.0 m depth), defined by the rapid decline of *M. insignilobus*-type (to 16–20%), the dominance of *C. ambigua* (20–60%) and high abundance of warmer-adapted shallow-water *Polypedilum nubeculosum*-type (7–17%) point to a clear-water lake phase and milder environmental conditions, similar to zone U15–C-2 of core A-KB 15/98 in deep-water sediments. These conditions in the littoral apparently facilitated the development of submerged macrophytes, such as the charophytes *C. hispida*, *Nitella hyalina*, and *Tolypella glomerata*, and the aquatic mosses *F. antipyretica* and *Scorpidium scorpioides*, numerous remains of which are recorded in the zone. An increase in habitat heterogeneity provided by the macrophytes favored changes in invertebrate assemblages, as evidenced by the high abundances of caddisflies (Trichoptera), alderflies (*Sialis*), oribatid mites (Oribatida), and freshwater molluscs (Gastropoda and Bivalvia) frequently associated with macrophyte-rich environments.

In the second half of zone U17–C-2 (31.0–30.3 m depth), the proportion of *C. ambigua* decreases down to 27%, whereas the proportion of shallow-water taxon *Microtendipes pedellus*-type increases towards the end of the zone up to 32%. The abundance of submerged macrophytes and associated invertebrates declines significantly, apparently due to the increased turbidity of the lake water.

The A-KB 16/98 section formed in the sublittoral zone (Fig. 2). Zone U16–C-1 (37.8–35.9 m depth) (Fig. 5) is marked by highest abundances of *C. ambigua* (41–55%). In the lowermost sample, its dominance together with the deep-water taxon *T. lugens*-type (14%) suggests a cool, low-productive clear-water environment, whereas in the next sample, its dominance together with high numbers of *C. anthracinus*-type (23%) and *E. pagana*-type (14%) suggests warmer and more productive conditions. The upper sample is also characterised by higher values of TOC (7 wt%) and $CaCO_3$ (55 im%).

Zone U16–C-2 (35.9–31.4 m depth), except the uppermost sample, is characterised by the prevalence of *P. penicillatus*-type (26–45%) typical of macrophyte-dominated conditions, overall increases in macrophyte-related *E. pagana*-type (10–32%) and *Tanytarsus glabrescens*-type (3–19%), high occurrences of other littoral chironomids and caddisflies, the presence of the charophyte alga *C. hispida* and the aquatic moss *F. antipyretica*, as well as by a high $CaCO_3$ content (28–62 im%). All of this implies an extension of the littoral zone, and mesotrophic conditions with clear water and submerged macrophytes. The presence of *Smittia foliacea*-type (1–7%), a semi-aquatic taxon with an affinity to ephemeral and marginal lake wetlands (Moller Pillot, 2008), can also be indicative of an increase in shoreline wetlands. The uppermost sample shows a return to colder, less productive conditions, as evidenced by the disappearance of submerged macrophytes, the rapid decline of *P. penicillatus*-type from the average percentage around 36%–5%, a

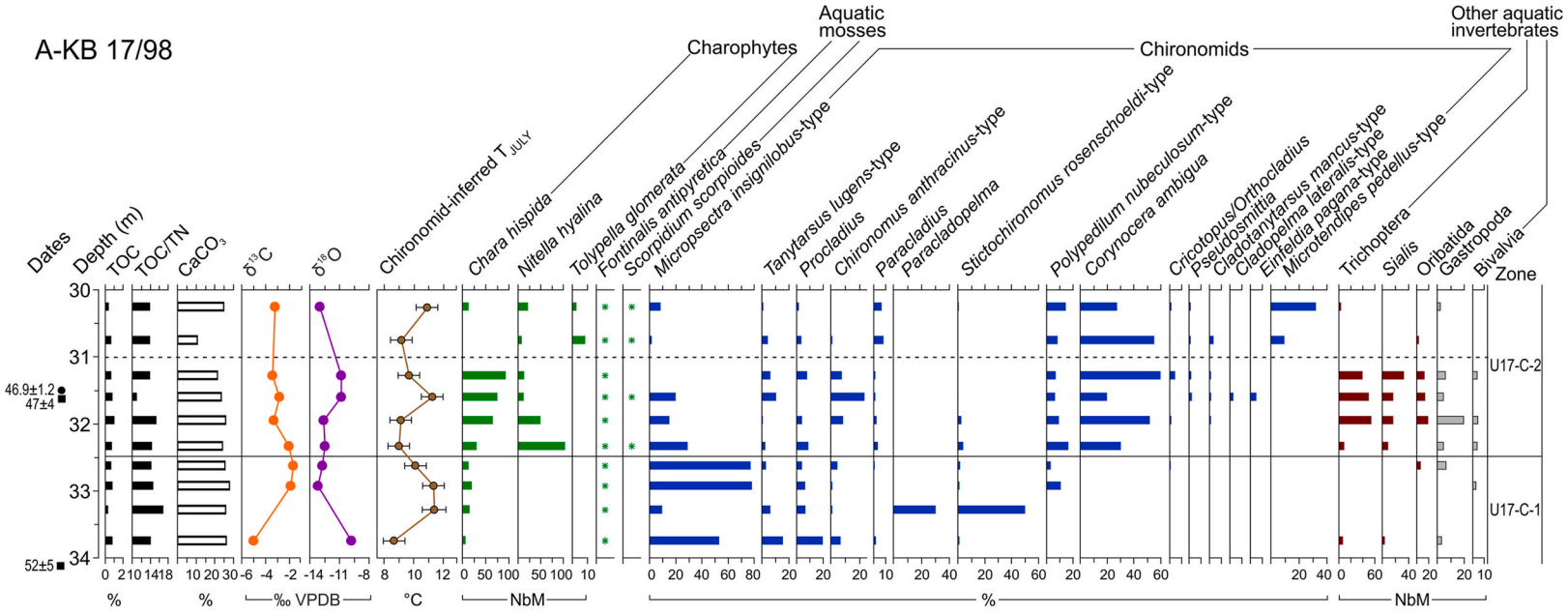


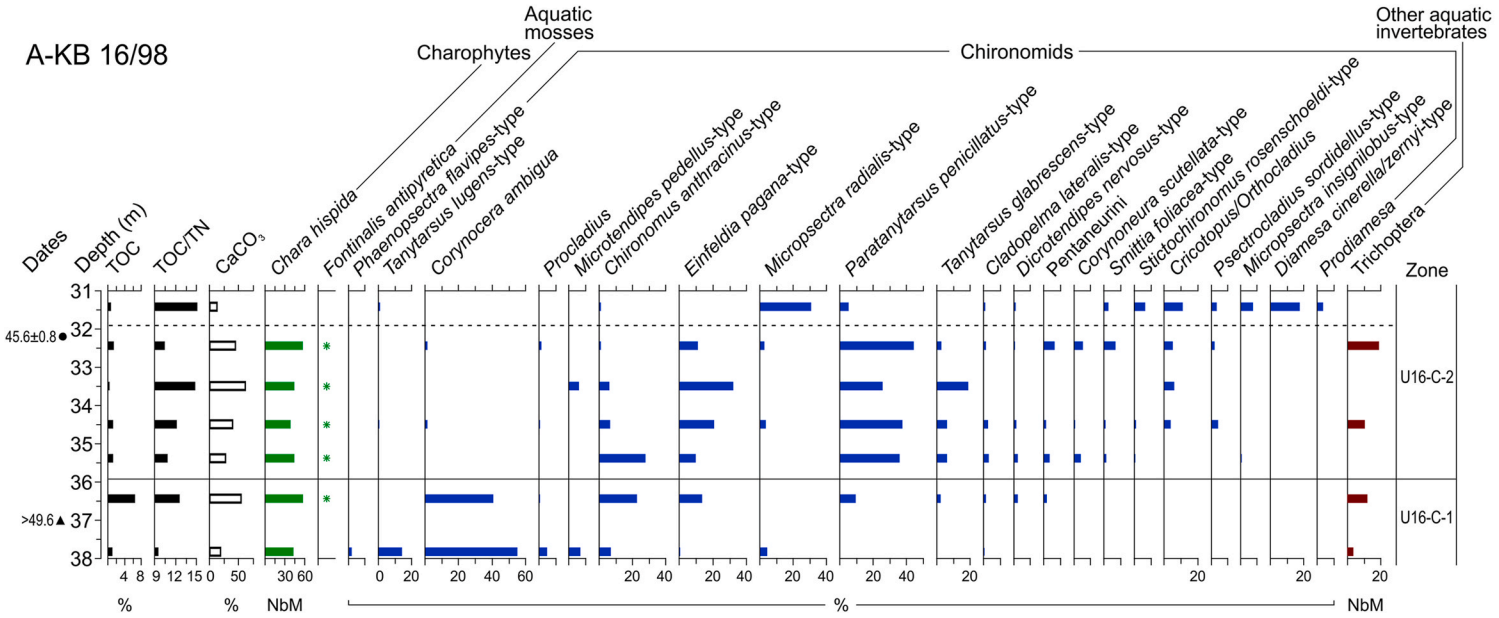


**Fig. 5.** Stratigraphy of the MIS 3 palaeolake deposit in cores A-KB 17/98 and A-KB 16/98. Legend as in Fig. 4. Selected dates from Starnberger et al. (2013a), abundance of subfossil remains of non-chironomid aquatic invertebrates, chironomid-inferred mean July air temperature ($T_{JULY}$) estimates plotted with sample-specific error bars and carbonate carbon ($\delta^{13}C$) and oxygen ($\delta^{18}O$) isotope data (core A-KB 17/98) are also presented. Dotted lines indicate the supposed shift from a clear-water to a turbid-water lake. Dates: OSL-dates (squares), calibrated (circles) and uncalibrated (triangle) radiocarbon ($^{14}C$) dates.

sharp increase of *M. radialis*-type (from ca. 3%–30%) and *S. rosenschoeldi*-type (from ca. 1%–6%), and the appearance of the cold stenotherm *Diamesa cinerella/zernyi*-type (18%) commonly living in either flowing water or littoral conditions of cold lakes (Makarchenko, 1985; Brooks et al., 2007).

#### 4.1.4. Cores A-KB 13/98 and A-KB 14/98, the northeast locations

The lacustrine sections of cores A-KB 13/98 and A-KB 14/98 from the northeast locations (Fig. 2) are characterised by higher carbonate contents of 55–88 im% (mean 70 im%) than the previously discussed sections (Fig. 6). TOC values are relatively low (1–2 wt%) and C/N ratios vary around 12–13, which are generally similar to those of the sediment sections from other locations in the palaeolake. Both sections are also marked by higher number of charophyte macrofossils; especially the section from core A-KB 14/98 exhibits an extremely high abundance of *C. hispida* oospores and gyrogonites.

The chironomid assemblages in both sections (Fig. 6) are characterised by a prevalence of taxa of the tribe Tanytarsini, such as warm-adapted and macrophyte-related *T. glabrescens*-type and *P. penicillatus*-type, as well as the typical inhabitant of clear-water lakes *C. ambigua*, which is abundant particularly in the uppermost samples. Also, *E. pagana*-type and chironomids of the tribe Pentaneurini, which commonly prefer littoral environments with soft sediments and abundant vegetation (Brodersen et al., 2001; Brooks et al., 2007), are present. Other shallow-water Tanytarsini (*Tanytarsus pallidicornis*-type 1, *T. mendax*-type, and *C. mancus*-type) and *Procladius*, as well as *Cricotopus/Orthocladius*, *Psectrocladius sordidellus*-type and *C. lateralis*-type, are recorded in the littoral sediments of core A-KB 13/98. The high presence of the ubiquitous free-ranging chironomid *Procladius* is interesting. Species of the genus *Procladius* tolerate low concentrations of dissolved oxygen (Quinlan et al., 1998) and often are present at greater depths together with species of the genus *Chironomus* (like in the A-KB 15/98 deep-water sediments, zone U15–C-1), which also tolerate low dissolved oxygen concentrations. On the other hand, the co-occurrence of *Procladius* and Tanytarsini in highly heterogeneous littoral habitats (like in the A-KB 13/98 littoral sediments) can point to very warm environments (Walker, 1995). Mandibles of larvae of the alderfly genus *Sialis*, which usually occur in muddy substrates with dead leaves, feed on small invertebrates and develop rapidly in warm, productive habitats (Anderson, 2009), are found in high numbers in a sample of core A-KB 14/98.

### 4.2. Oxygen and carbon isotope records (cores A-KB 17/98 and A-KB 13/98)

Calcium carbonate precipitation resulting from photosynthetic activity of charophytes is most intensive within the littoral zone during summertime (Pełechaty et al., 2013). Stable oxygen ($\delta^{18}O$) and carbon ($\delta^{13}C$) isotope values of lacustrine carbonates are common proxies in

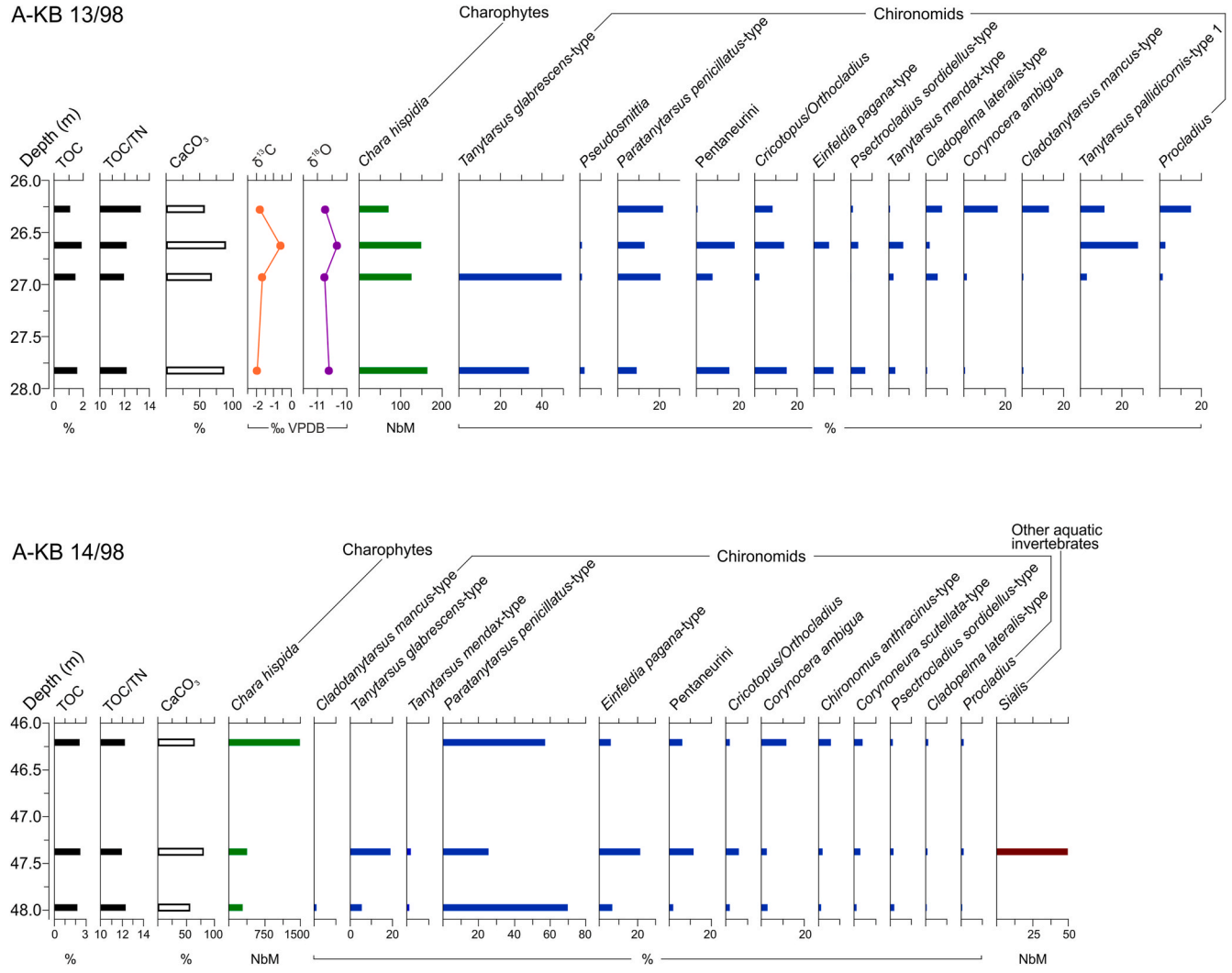


**Fig. 6.** Stratigraphy of the MIS 3 palaeolake deposits in cores A-KB 13/98 and A-KB 14/98. Legend as in Fig. 4. Abundance of subfossil remains of non-chironomid aquatic invertebrates in the cores and carbonate carbon ($\delta^{13}C$) and oxygen ($\delta^{18}O$) isotope records from core A-KB 13/98 are also presented.

palaeolimnological studies, providing information on climate change and environmental dynamics. The $\delta^{18}O$ composition of carbonates formed in hardwater lakes is dependent both on the water temperature and its isotopic composition, which is in turn related to the isotopic composition of precipitation and the hydrologic regime of the lakes (Leng and Henderson, 2013). Carbonate $\delta^{13}C$ values reflect the photosynthetic activity of aquatic primary producers, the isotopic composition of inflowing waters as well as evaporation and $CO_2$ exchange between the lake water and the atmosphere (Leng and Marshall, 2004).

Core A-KB 17/98 from the southwest part of the lake offers more detailed isotopic records then core A-KB 13/98 from the northeast part (Figs. 5 and 6). Warmer waters precipitate calcite of lower $\delta^{18}O$ values due to temperature-dependent isotope fractionation (Jonsson et al., 2010). Hence the pronounced decrease in $\delta^{18}O$ from −10‰ in the lowermost sediment (33.8 m depth) to −13‰ at 32.9 m depth in core A-KB 17/98 may reflect an increase in summer water temperature after the filling the lake basin with snow/glacier meltwater.

The $\delta^{18}O$ values show a gradual increase from −13‰ to −11‰ over the range from 32.9 to 31.3 m depth (Fig. 5), suggesting an increased impact of evaporative $\delta^{18}O$ enrichment of the lake water induced by an increase in the evaporation/inflow ratio of the basin and/or prolonged water residence time in the lake. Also, an increase in $\delta^{18}O$ in precipitation could have contributed to the observed increase.

The decline in $\delta^{18}O$ from −11‰ (31.3 m depth) to −13‰ in the topmost sample (30.3 m depth) may be attributed to a warming-induced input of $^{18}O$-depleted snow/glacial meltwater into the lake, as suggested by the changes in macrophyte and invertebrate assemblages (see section 4.1 for more details). Hydrologic factors of local significance, such as runoff, stream and groundwater inflow, and evaporation also control the isotopic composition of lacustrine carbonates and may sometimes be more important than large-scale changes in atmospheric circulation and mean annual air temperature (Hammarlund, 1994; Ito, 2001).

The lowest $\delta^{13}C$ value of −5‰ in the lowermost sediment suggests a very low productivity level and a dominant role of respiration in the lake during the initial time of lacustrine deposition, resulting in less intensive removal of $^{12}C$ from the dissolved inorganic carbon of the lake water by phytoplankton via photosynthesis and/or high rates of release of $^{12}C$ during respiratory processes. The increase in $\delta^{13}C$ to −2‰ at 32.9 m depth points to increased photosynthetic activity in the lake in response to either elevated $CO_2$ and/or temperature, giving rise to $^{13}C$-enrichment of dissolved inorganic carbon. Enhanced dissolution of carbonates in the catchment under increasing surface runoff, as well as a longer residence time and enhanced isotopic exchange with relatively $^{13}C$-enriched atmospheric carbon dioxide may also have played a role.

$\delta^{13}C$ exhibits relatively stable values around −2‰ at 33.0–32.3 m depth, which are the maximum values of the studied section. The $^{13}C$-enrichment suggests elevated aquatic productivity. The drop in average $\delta^{13}C$ values to −3‰ at 32.3–32.0 m depth could suggest a decline in photosynthetic activity in the lake. On the other hand, in more mature lake ecosystems with high macrophyte biomass, decomposition of organic material may lead to a relative depletion of $\delta^{13}C$ in dissolved inorganic carbon even when vegetation production is increased or generally high (cf. Hammarlund, 1994). Therefore, the lowered carbonate $\delta^{13}C$ values may also be caused by increased recycling of $^{13}C$-depleted carbon dioxide derived from decaying plant tissues. Relatively stable values around −3‰ persist through the rest of the record (32.0–30.3 m depth).

The $\delta^{18}O$ and $\delta^{13}C$ values show a negative covariance ($r = -0.75$; $p \leq 0.05$) over the length of the record, suggesting that open-basin conditions prevailed for the majority of the period and that precipitation and evaporation were not the dominant processes determining the hydrologic and isotopic balance of the lake (Talbot, 1990; Horton et al., 2016). Water temperature and hydrologic factors are regarded here as more important in controlling the oxygen and carbon isotope composition of the endogenic carbonates.

In core A-KB 13/98 from the littoral area in the northeast part of the lake, which contains exceptionally calcite-rich sediments (marls), the $\delta^{18}O$ and $\delta^{13}C$ values scatter around −10.6‰ and −1.5‰, respectively (Fig. 6). The relatively high $\delta^{18}O$ and $\delta^{13}C$ values suggest a high photosynthetic activity of macrophytes in this part of the lake.

### 4.3. Chironomid-based summer air temperatures (cores A-KB 15/98 and A-KB 17/98)

The mean July air temperature estimates based on the chironomid data from the deep-water core A-KB 15/98, for which the age-depth model was developed, reveal an amplitude of ca. 5°C over the study period (Fig. 7). Inferred temperatures show very little change within zone U15–C-1 (ca. 54.6–52.2 cal ka BP), fluctuating around 8.5°C within a range of 8–9°C. Throughout the most productive zone U15–C-2, there are distinct time episodes of warmer and cooler temperatures. The onset of the zone displays a steady increase in temperature reaching 11°C at ca. 50.8 cal ka BP. After a return towards cooler conditions as indicated by a sample at ca. 50.3 cal ka BP with an inferred temperature of ca. 9°C, temperatures increased again and remained stable at around 11°C until ca. 47.7 cal ka BP. This is followed by a distinct decrease to values averaging around 9.5°C with such cooler temperatures persisting until ca. 45 cal ka BP. The next samples show a return towards warmer conditions between ca. 44.1 and 43.3 cal ka BP, tentatively correlated with Greenland Interstadial (GI) 11, with temperatures increasing to the maximum inferred values of around 12.5°C (Fig. 8). In Zone U15–C-3, temperatures declined and stabilised around 10–11°C up to the end of the record at 41.5 cal ka BP.

All taxa found in the down-core samples, except for the low-abundance *Constempellina* (1.4%) found only in the lowermost sample, are well represented in the modern training set used to develop the applied chironomid-temperature transfer function. Only one sample (17.2 m depth) shows a 'no good' analogue in the modern data and also has a residual chi-square distance higher than the extreme 10% of the modern samples and therefore is classified as having a 'poor' fit with temperature.

The sample providing the highest temperature inference (17.2 m depth; 12.7°C) of the entire record is characterised by the occurrence of the warm-adapted *Stempellina* (Brooks et al., 2007; Heiri and Lotter, 2010) at a greater abundance (7.4%) than its maximum value in the training set (4.3%) and therefore shows no modern analogue. However, WA-PLS regression and calibration based on the optima of the taxa included in the model perform relatively well in poor analogue situations (Birks, 1998), interpolating temperature estimates for assemblages consisting of taxa that do not coexist in the modern training set samples. A 'poor' fit to temperature in this sample may be related to a relatively high abundance (11.1%) of *Limnophyes/Paralimnophyes* which is characterised by very broad distributions with respect to temperature in the training set (Heiri et al., 2011). Larvae of these taxa commonly inhabit the margins and shallow zones of lakes and are frequently associated with aquatic plants (Janecek et al., 2002; Brooks et al., 2007). Another taxon, the warm-adapted *Stempellina,* requires coarse, grainy substrates, like sand, to construct its casings and can occur in cooler lakes where it likely responds to substrate rather than temperature (Rees et al., 2008). This evidence suggests that variables other than temperature may have influenced the response of the chironomid assemblage at that time, and therefore, the temperature inference should be treated with caution. Remarkably, the nearby sample (16.9 m depth), which shows a 'good' modern analogue and has a high goodness-of-fit to temperature, provides a temperature (12.3°C) very close to that of the previous sample (17.2 m depth; 12.7°C) with poor reconstruction diagnostics.

One more sample (at 18.5 m depth) has a 'very poor' fit with temperature, most probably related to the presence of *Georthocladius* (1.2%), which prefers semi-aquatic/terrestrial habitats (Brooks et al., 2007; Polášková et al., 2020) and is relatively rare in the inference model (Heiri et al., 2011). However, the abundance of this taxon is low and the temperature inference of this sample is in a part of the record

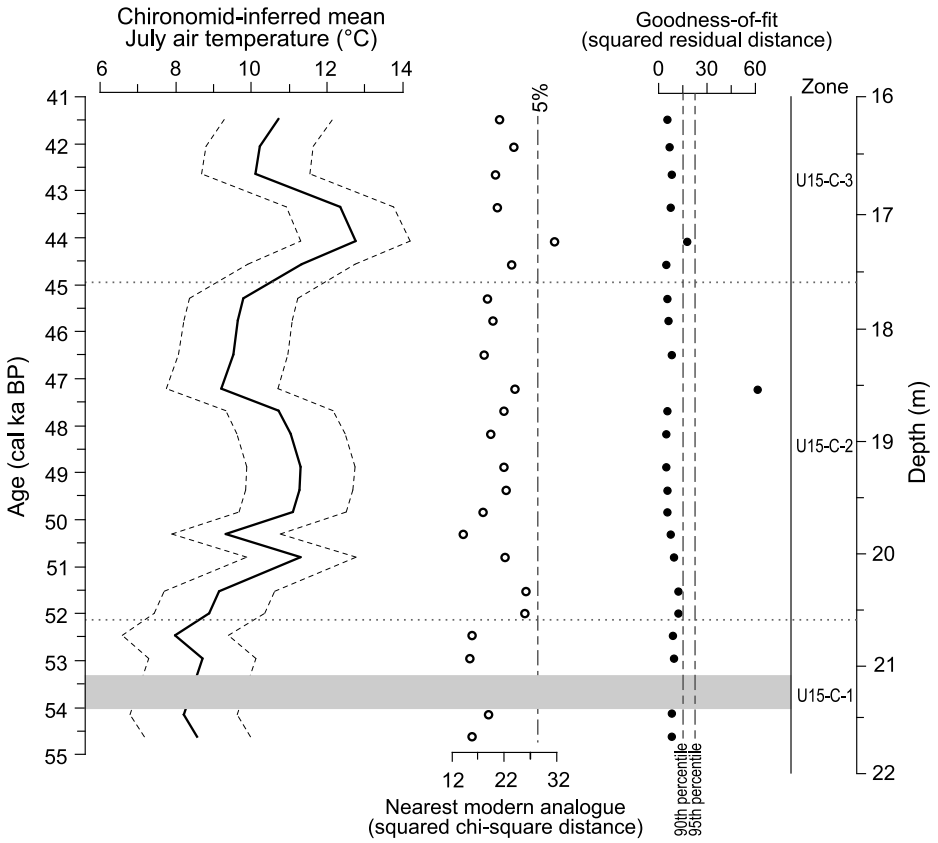


**Fig. 7.** Chironomid-inferred mean July air temperature (solid line) from core A-KB 15/98 plotted together with sample-specific standard errors of prediction (dashed lines), and reconstruction diagnostic statistics such as nearest modern analogues for the fossil samples in the calibration data set, and goodness-of-fit statistics of the fossil samples with temperature. Vertical dashed lines are used to identify samples with 'no good' (5%) modern analogues, and samples with 'poor' (90th percentile) and 'very poor' fit (95th percentile) with temperature. Horizontal dotted lines mark chironomid assemblage zones. Grey band indicates an interval lacking chironomid subfossils.

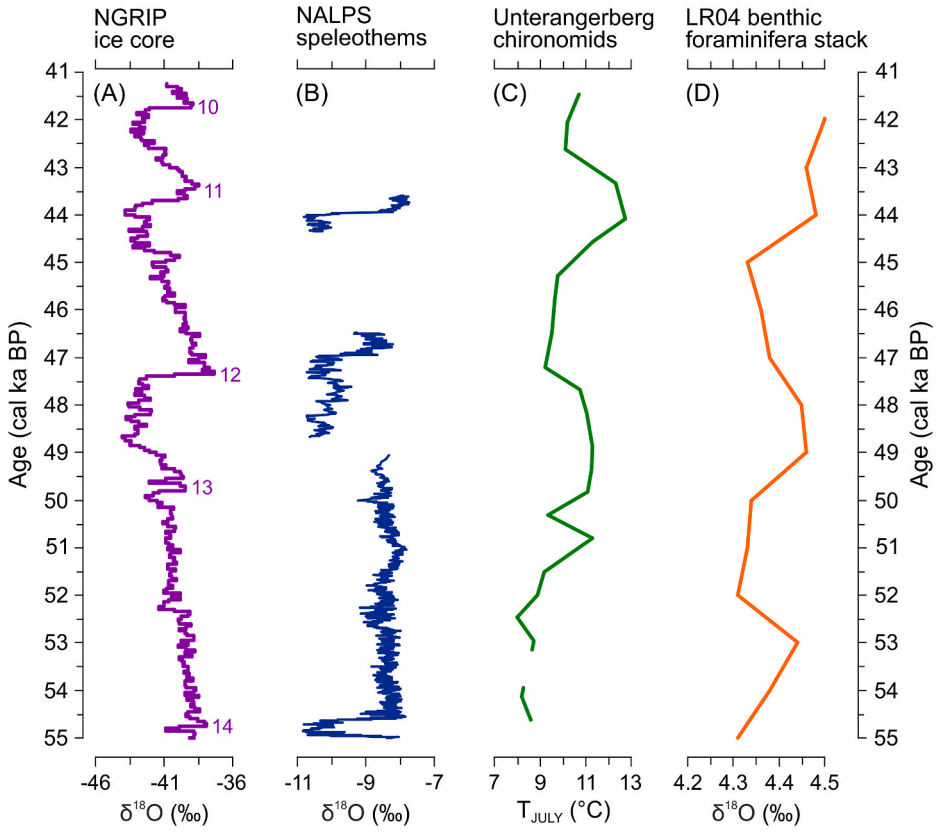


**Fig. 8.** Comparison of the Unterangerberg temperature reconstruction with other climate records. (A) NGRIP oxygen isotope record from Greenland ice core (North Greenland Ice Core Project Members, 2004). Numbers denote Greenland Interstadials. (B) Northern Alps (NALPS) speleothem oxygen isotope record (Hölloch cave; Moseley et al., 2014). (C) Chironomid-inferred mean July air temperature ($T_{JULY}$) estimates at Unterangerberg (this study). (D) LR04 benthic foraminifera oxygen isotope stack (Lisiecki and Raymo, 2005).

where the reconstructed temperatures are stable.

The temperature reconstruction derived from the A-KB 17/98 chironomid data is presented in Fig. 5. We do not discuss these temperature inferences in detail since the sediments originated in the littoral zone and this part of the core does not have a sufficient number of dates for constructing an age–depth model. The general pattern of chironomid-inferred temperature changes, however, exhibits alternating warming and cooling trends and resembles stadial-interstadial temperature variations characteristic of MIS 3. The record indicates minimum (stadial) July air temperatures of around 9°C and maximum (interstadial) ones close to 11.5°C, corresponding, in general, to the estimates inferred from the chironomid assemblages of core A-KB 15/98 from deeper waters of the palaeolake.

## 5. Discussion

The palaeolake of Unterangerberg was elongated and about 3–4 km long and occupied a SW-NE oriented depression during the first half of MIS 3 (Starnberger et al., 2013a). Comparing the elevations of the topmost lake sediments (Fig. 2) in the littoral core A-KB 17/98 (ca. 604 m a.s.l.) from the southwest part of the lake and the deep-water core A-KB 15/98 (ca. 582 m a.s.l.) from the central part of the lake implies a maximum water depth of no more than 20 m (Starnberger et al., 2013a). Sedimentation rates in lakes are typically highest in areas near the mouth of a stream/river entering the lake. These deltaic areas are characterised by thick deposits that are topographically heterogeneous and therefore support varied vegetation and invertebrates (Smith, 1991) and are distinguished by extremely high levels of biodiversity and productivity (Tockner and Stanford, 2002). The littoral cores A-KB 17/98 and A-KB 16/98 in the southwest part of the Unterangerberg lake are characterised by a much greater thickness of the lacustrine deposits (ca. 5 and 7 m, respectively) as well as species richness and structural complexity of the macrophyte and invertebrate assemblages (Fig. 5) than the littoral core A-KB 13/98 in the northeast part with 2 m thick sequence of lacustrine deposits (Fig. 6). This suggests that the lake had an inlet stream at its southwestern end and acted as an open-basin system.

The comparison of the distribution of subfossil macrophyte and invertebrate assemblages in the cores along the SW–NE transect in the palaeolake with depths of up to 20 m and an inlet stream at its southwestern end highlighted differences that are obviously linked to the depth- and area-specific changes in the assemblages over time. The integration of the biotic and abiotic proxy data from all available sediment cores allows reconstructing the environmental history of the palaeolake throughout the first half of MIS 3.

### 5.1. Lake environments and catchment vegetation

The appearance and dominance of lacustrine chironomid taxa in the sample at ca. 54.6 cal ka BP mark the onset of lacustrine conditions in the Unterangerberg basin at this period (Fig. 4). This timing is tentatively correlated with the start of GI 14, the longest D/O warm phase in Greenland during MIS 3 (Rasmussen et al., 2014). Stalagmite records in the Alps recorded the onset of this interstadial at 54.5 ka BP, synchronous with the warming in Greenland (Spötl et al., 2006; Moseley et al., 2014) (Fig. 8).

The pioneer chironomid assemblages (ca. 54.6–52.2 cal ka BP; zones U15–C-1 and U17–C-1) with the prevalence of cold-adapted taxa reflect a cold, oligotrophic and relatively deep lake ecosystem. The deep-water habitats were dominated by the true cold-stenotherm *M. radialis*-type, typical of lakes situated both at high altitudes (above 2000 m a.s.l.) and at high latitudes, while the littoral habitats were dominated by *M. insignilobus*-type, commonly abundant in lakes at intermediate altitudes and subarctic regions (Heiri et al., 2011). Low TOC levels in the sediments corroborate the chironomid data for this period, revealing a nutrient-poor lake with low primary productivity. Scarce remains of only aquatic mosses (core A-KB 17/98) point to a nearly macrophyte-free lake during this period. Pollen-based inferences (Starnberger et al., 2013a; zone LPZ KB 17–6) corresponding to zone U17–C-1 indicate an open vegetation in the catchment with scattered individual trees or small tree stands (*Betula*, *Pinus*, *Picea*), a modest shrub flora and low diversity of herb species.

Core A-KB 15/98 revealed a change in the environment around ca. 53.8 cal ka BP with the disappearance of the aquatic biota. This marks the cessation of lacustrine deposition at Unterangerberg, suggesting the interruption of relatively warm conditions during the early interstadial and probably a temporary return to harsh environmental conditions. A similar interval (between ca. 53 and 54 ka BP), during which chironomids and other aquatic invertebrates were absent, suggesting a major climate shift, has been observed in Füramoos in the Alpine foreland of southern Germany (Bolland et al., 2021a). Rock flour layers in the Nesseltalgraben record of Berchtesgaden on the northern rim of the Alps indicate the advance of a local glacier around 52–51 cal ka BP (Mayr et al., 2019), but this difference is within the uncertainty range of the chronologies. This climate pattern may signal a regional signature of climate cooling and advances of glaciers at that time.

The next phase (ca. 52.2–44.9 cal ka BP; zones U15–C-2, U17–C-2 and U16–C-1) was characterised by a clear-water, macrophyte-dominated state. *C. ambigua*, which is absent from the present-day fauna of the Alpine region (Heiri et al., 2011), dominated this interval. This species is often associated with charophytes, likely because of similar physical and chemical requirements (see section 3.1.1 for more details). Overall, the chironomid assemblages suggest warmer and more productive conditions. Apparently, the lake water chemistry continued to be mainly determined by the local geology, namely carbonate-rich till and carbonate bedrock. Clear hardwater conditions favored a larger depth of the euphotic zone allowing for a major proportion of the lake floor to be occupied by submerged macrophytes, mainly charophytes. The rapid expansion of submerged vegetation at the start of this phase provided a refuge for a wide diversity of aquatic invertebrates. An increased productivity of the lake is indicated by a higher TOC content in the deep-water sediments and by the C/N values (8–13) suggesting that macrophytes were a major contribution of organic matter to the lake sediments and that terrestrial input was low.

The sediments from the littoral and sublittoral locations contain less organic matter and more $CaCO_3$ than deep-water sediments, which is typical for hardwater lakes (Dean, 1999). Charophytes, due to their capacity to assimilate soluble bicarbonates during photosynthesis and to convert them into insoluble calcium carbonate, deposited onto the thallus and oospore surfaces as mineral encrustations, are highly effective in the deposition of calcium carbonate in lake sediments (Pełechaty et al., 2013). Numerous charophyte encrustations were found in the littoral and sublittoral sediments deposited over this time period. Warmer climate and a concomitant increase in water temperature promote charophyte production (Choudhury et al., 2019) and thereby drive calcite precipitation forming calcite-rich sediments (marls) during interglacials or interstadials (Jones et al., 2002; Vogel et al., 2010; Wiik et al., 2013).

Pollen data from Unterangerberg indicate the existence of a dense forest (arboreal pollen exceeding 80%) dominated by *Betula* with the presence of *Pinus cembra* at the beginning of this period (Starnberger et al., 2013a; zone LPZ KB 15–2). Afterwards, there was a gradual retreat of trees and shrubs (arboreal pollen <40%) in favour of grasses, sedges and heliophilous herbs (Starnberger et al., 2013a; zones LPZ KB 15–3 and LPZ KB 17–7). Such a vegetation change in the catchment during MIS 3 interstadials with mild summers may have been a response to reduced summer precipitation, too low number of growing degree days (with a baseline of 5°C) and/or frequent killing frosts (Van Meerbeeck et al., 2011).

The following phase (ca. 44.9–41.5 cal ka BP; zones U15–C-3 and U16–C-2) is marked by a low level of biological productivity in the lake, inferred by low TOC values and low abundances of chironomids. The

coexistence of chironomid taxa typical of cool environments and the ones associated with more temperate conditions during this phase may have be related to climate instability. The substantial decrease in the abundance of submerged macrophytes and associated invertebrates at the start of the phase suggests a regime shift in the lake, from a clear-water to a turbid-water state in which the macrophyte growth was highly restricted and water turbidity was elevated. The main controlling factor for the two alternative states is the turbidity of water regulating the vertical light penetration (Scheffer, 1990). This regime shift coincides with the highest temperatures inferred from the Unterangerberg chironomid data (Fig. 8) and roughly corresponds to the warming of GI 11 marked in the Northern Alps speleothem record (Moseley et al., 2014). Apparently, the elevated turbidity of the lake water was the result of enhanced melting of glaciers situated on the nearby mountain ranges. A related increased meltwater supply, containing high amounts of suspension load, to the headwater stream flowed into the south-western end of the lake shifted the ecosystem to the alternative state. In the turbid state, high concentrations of particulate matter affected light penetration, which in turn, restricted the growth and distributions of submerged macrophytes. Since the particle content of lake water gradually decreases with increasing distance from a river/stream mouth, the northeast part of the lake, which is furthest from the supposed inlet stream, was least affected by suspension-rich water. It is noteworthy that a prolonged period (46.3–42.9 cal ka BP) of meltwater input has also been recorded in the Nesseltalgraben record, ca. 100 km east of the Unterangerberg terrace (Mayr et al., 2019).

Pollen data (Starnberger et al., 2013a; the upper part of zone LPZ KB 15–3) point to the development of a more open vegetation (arboreal pollen <20%) dominated by herbs during this phase. The spread of Alpine tundra vegetation after 43 cal ka BP has also been recorded at the Nesseltalgraben site (Stojakowits et al., 2020).

The MIS 3 lacustrine sedimentation ended ca. 41.5 cal ka BP with the deposition of sand and gravel. The lake ceased to exist likely due to a substantial transformation of the regional hydrological system as a consequence of climate-induced intensification of (peri)glacial processes.

### 5.2. Pattern of temperature changes during MIS 3

The chironomid-based temperature record from Unterangerberg covers the period between ca. 54.6 and 41.5 cal ka BP and provides evidence of millennial-scale climate variability during the first half of MIS 3 (Figs. 7 and 8). The early part of the record (ca. 54.6–52.2 cal ka BP) concurrent with most of GI 14, the longest interstadial in MIS 3, was characterised by mean July air temperatures of 8–9°C. These inferred temperatures may, however, be underestimated because of snow/glacier meltwater that filled the lake. An indirect influence of climate change, related to increased meltwater input into the lake basin early in the interstadial, is also supported by the oxygen isotope data. In these situations, the lake water temperature is decoupled from air temperature and lakes support chironomid assemblages typical of temperatures colder than expected from the local air temperature (Brooks and Birks, 2001; Engels et al., 2008a). By the end of the interstadial (ca. 51 cal ka BP), when the relationship between air and water temperatures in the lake became stronger, the inferred temperatures increased to ca. 11°C.

A decrease in temperature to ca. 9°C is recorded at ca. 50.3 cal ka BP and likely corresponds to the stadial following GI 14. After this cold reversal, temperatures increased and remained stable around 11°C until ca. 47.7 cal ka BP after which they declined again to ca. 9°C at ca. 47.2 cal ka BP. Afterwards the data suggest an increase to ca. 12.5°C at ca. 44.1–43.3 cal ka BP followed by a decrease up to ca. 10°C between ca. 42.6 and 41.5 cal ka BP. This pattern is reminiscent of stadial/interstadial temperature changes, although a precise correlation with e.g. events recorded in the Greenland ice cores is hampered due to the low resolution of the lake sediment archive and significant age uncertainties. Nevertheless, the warm phases between ca. 50.0 and 47.7 cal ka BP, and between ca. 44.1 and 43.3 cal ka BP may be tentatively assigned to GI 13 and GI 11, respectively, whereas GI 12 is not clearly recorded.

The chironomid-based climate reconstructions suggest mean July air temperatures during interstadials between ca. 11.0 and 12.5°C (i.e. ca 5–6°C below present-day values) and ca. 9–10°C during stadial episodes (i.e. ca 7–8°C below present-day values). In MIS 3 climate simulations, stadials and interstadials differs only very slightly (by ca. 1°C) both in summer and winter and the stadial climate is not cold enough to represent stadial conditions in Europe (Van Meerbeeck et al., 2009). Chironomid-inferred temperatures at Unterangerberg suggest differences of ca. 2°C in July temperatures between MIS 3 interstadials and stadials. This corroborates findings from other studies (e.g. Denton et al., 2005; Helmens, 2014) that summer temperature changes during D/O events were relatively modest whereas major shifts in temperature values occurred during wintertime. Given that at present the minimum mean July air temperature for the growth of tree species in the Alps is ca. 8–10°C (Landolt, 1992), evidence of steppe-tundra vegetation at the study site during the MIS 3 stadials (Starnberger et al., 2013a) points to a pronounced seasonality with relatively mild but short summers and strong winter cooling which may have prevented trees from growing in this inner-Alpine valley.

Studies based on subfossil beetle assemblages from the lower lignite of the Gossau interstadial complex (Jost-Stauffer et al., 2005) and the interstadial section of the mammoth peat at Niederweningen (Coope, 2007), both located in the northern Swiss Alpine foreland, dated to ca. 45 ka BP and tentatively correlated to GI 12 (Hajdas et al., 2007; Furrer et al., 2007), provide mean July air temperature estimetes of ca. 12–13°C. The chironomid record from Füramoos in the northern foreland of the Eastern Alps (southern Germany) indicates similar estimates of July temperatures (11–12°C) for the Bellamont 1 interstadial phase (ca. 53–49 ka BP) correlated to GIs 14 and 13 (Bolland et al., 2021a). These inferences fall well within the range of interstadial July temperatures inferrred from the chironomid assemblages at Unterangerberg (11–12.5°C). Altogether, these reconstructions indicate that climatic conditions in the Alps and their northern foreland were relatively mild during interstadial summers but significantly cooler than today, with July temperatures ca. 5–6°C below present-day values.

The lacustrine sedimentation at Unterangerberg was terminated ca. 41.5 cal ka BP. Also, peat formation at Niederweningen stopped and sedimentation at Gossau was interrupted by about 42 ka BP (Furrer et al., 2007; Hajdas et al., 2009). According to a recent study, the Laschamps geomagnetic reversal (42.2–41.5 cal ka BP) combined with Grand Solar Minima may have triggered global climate shifts that could have had widespread impacts on natural systems as well as humas (Cooper et al., 2021). Across Europe, climate change in the late MIS 3 led to dramatic changes in glacier extent and sea level with major impacts on the physiography of mountain areas, coastal regions and hydrologic systems (Badino et al., 2020).

## 6. Conclusions

This study provides a multiproxy record from a palaeolake that existed on the inner-Alpine valley terrace of Unterangerberg in the Eastern Alps during the first half of MIS 3. Lacustrine deposits were examined in five drill cores. The biotic and abiotic proxies indicate the onset of lacustrine sedimentation at ca. 54.6 cal ka BP, i.e. at the beginning of GI 14. In the initial stage (ca. 54.6–52.2 cal ka BP), the lake was a cold, oligotrophic water body influenced by snow/glacier meltwater. The cessation of lacustrine deposition in the basin suggests a temporary return to harsh environmental conditions at ca. 53.8 cal ka

BP. In the next phase (ca. 52.2–44.9 cal ka BP), a great proportion of the lake floor was occupied by submerged macrophytes (charophytes and aquatic mosses) and the lake apparently was in a clear-water, macrophyte-dominated state. The chironomid *Corynocera ambigua*, a species absent from the present-day fauna of the Alpine region, dominated this interval. Marl deposition reflecting high limnic productivity occurred under warm-summer interstadial conditions. A much greater thickness of the lacustrine deposits and a greater structural complexity of the macrophyte and invertebrate assemblages in the southwest part of the lake than in its northeast part suggest that the lake had an inlet stream in the southwest. In the following phase (ca. 44.9–41.5 cal ka BP) the lake was characterised by overall low productivity and the coexistence of chironomid taxa typical of cold environments and others associated with more temperate environments. The drastic reduction in the abundance of submerged macrophytes and associated invertebrates at the start of this phase suggests a shift from a clear-water to a turbid-water lake. Enhanced input of glacier meltwater from the nearby mountains may have resulted in elevated turbidity of the lake water. This lacustrine regime was terminated ca. 41.5 cal ka BP, apparently because of a substantial change of the regional hydrological system.

Quantitative estimates based on chironomids suggest that mean July air temperatures were between 11 and 12.5°C during interstadials and 9–10°C during stadials, revealing differences in summer temperatures of ca. 2°C between warmer and colder periods of MIS 3. Relatively mild interstadial summers were much cooler than today, with July temperatures ca. 5–6°C below present-day values, which corroborates findings from other sites in the Alps.

## Author contributions

EAI: conceptualization, methodology, formal analysis, investigation, data curation, writing – original draft, visualization, funding acquisition, and project administration. BPI: conceptualization, methodology, investigation, visualization, writing – original draft, review & editing. OH: methodology, validation, formal analysis, writing – review & editing. CS: conceptualization, methodology, investigation, writing – review & editing.

## Declaration of competing interest

The authors declare that they have no known competing financial interests or personal relationships that could have appeared to influence the work reported in this paper.

## Acknowledgements

This research was funded by the Austrian Science Fund (FWF; project number P 28469-B25) awarded to EAI. BPI acknowledges financial support from by the Austrian Science Fund through FWF grant P 33786-N. OH has been supported by the Swiss National Science Foundation (SNSF, grant 200021_165494). The authors are grateful to Reinhard Starnberger and Karin Koinig for drawing our attention to the site and for their assistance during core inspection and sampling. We further thank Gry Larsen for technical support in the laboratory. We are also grateful to François Bochereau for assistance with the nitrogen and carbon measurements at the Forest Research Laboratory (Farnham, UK). We would like to express our great appreciation to Heinz Furrer for helpful advice, which led to improvements in this paper.

## References

Chironomidae of the holarctic region. Keys and diagnoses – larvae. In: Andersen, T., Cranston, P.S., Epler, J.H. (Eds.), Insect Systemat. Evol. Suppl. 66, 1–571.

Anderson, N.H., 2009. Megaloptera. In: Resh, V.H., Cardé, R.T. (Eds.), Encyclopedia of Insects, second ed. Academic Press/Elsevier, London, pp. 620–623.

Badino, F., Pini, R., Ravazzi, C., et al., 2020. An overview of Alpine and Mediterranean palaeogeography, terrestrial ecosystems and climate history during MIS 3 with focus on the Middle to Upper Palaeolithic transition. Quat. Int. 551, 7–28. https://doi.org/10.1016/j.quaint.2019.09.024.

Barley, E.M., Walker, I.R., Kurek, J., Cwynar, L.C., Mathewes, R.W., Gajewski, K., Finney, B.P., 2006. A northwest North American training set: distribution of freshwater midges in relation to air temperature and lake depth. J. Paleolimnol. 36, 295–314. https://doi.org/10.1007/s10933-006-0014-6.

Barrett, S.J., Starnberger, R., Tjallingii, R., Brauer, A., Spötl, C., 2017. The sedimentary history of the inner-alpine Inn Valley (Austria): extending the Baumkirchen type section further back in time with new drilling. J. Quat. Sci. 32, 63–79. https://doi.org/10.1002/jqs.2924.

Becker, A., Ammann, B., Anselmetti, F.S., Hirt, A.M., Magny, M., Millet, L., Rachoud, A. M., Sampietro, G., Wüthrich, C., 2006. Paleoenvironmental studies on lake Bergsee, Black Forest, Germany. Neues Jahrbuch Geol. Palaontol. Abhand. 240, 405–445.

Bennett, K.D., 1996. Determination of the number of zones in a biostratigraphical sequence. New Phytol. 132, 155–170. https://doi.org/10.1111/j.1469-8137.1996.tb04521.x.

Bennett, K.D., 2009. Documentation for Psimpoll 4.27 and pscomb 1.03. C programs for plotting and analyzing pollen data. In: The 14Chrono Centre, Archaeology and Palaeoecology. Queen's University of Belfast, Belfast.

Birks, H.J.B., 1998. Numerical tools in paleolimnology: progress, potentialities and problems. J. Paleolimnol. 20, 307–332. https://doi.org/10.1023/A:1008038808690.

Birks, H.J.B., Line, J.M., Juggins, S., Stevenson, A.C., ter Braak, C.J.F., 1990. Diatoms and pH reconstruction. Philos. Trans. R. Soc. London, Ser. A B 327, 263–278. https://doi.org/10.1098/rstb.1990.0062.

Birks, H.J.B., Heiri, O., Seppä, H., Bjune, A.E., 2010. Strengths and weaknesses of quantitative climate reconstructions based on late-Quaternary biological proxies. Open J. Ecol. 3, 68–110. https://doi.org/10.2174/1874213001003020068.

Böhm, R., Auer, I., Brunetti, M., Maugeri, M., Nanni, T., Schöner, W., 2001. Regional temperature variability in the European Alps: 1760–1998 from homogenized instrumental time series. Int. J. Climatol. 21, 1779–1801. https://doi.org/10.1002/joc.689.

Bolland, A., Kern, O.A., Allstädt, F.J., Peteet, D., Koutsodendris, A., Pross, J., Heiri, O., 2021a. Summer temperatures during the last glaciation (MIS 5c to MIS 3) inferred from a 50,000-year chironomid record from Füramoos, southern Germany. Quat. Sci. Rev. 264, 107008. https://doi.org/10.1016/j.quascirev.2021.107008.

Bolland, A., Kern, O.A., Koutsodendris, A., Pross, J., Heiri, O., 2021b. Chironomid-inferred summer temperature development during the late Rissian glacial, Eemian interglacial and earliest Würmian glacial at Füramoos, southern Germany. Boreas. https://doi.org/10.1111/bor.12567.

Brodersen, K.P., Lindegaard, C., 1999. Mass occurrence and sporadic distribution of Corynocera ambigua Zettersedt (Diptera, Chironomidae) in Danish lakes. Neo and palaeolimnological records. J. Paleolimnol. 22, 41–52. https://doi.org/10.1023/A:1008032619776.

Brodersen, K.P., Odgaard, B., Vestergaard, O., Anderson, N.J., 2001. Chironomid stratigraphy in the shallow and eutrophic Lake Søbygaard, Denmark: chironomid-macrophyte co-occurrence. Freshw. Biol. 46, 253–267. https://doi.org/10.1046/j.1365-2427.2001.00652.x.

Bronk Ramsey, C., 2008. Deposition models for chronological records. Quat. Sci. Rev. 27, 42–60. https://doi.org/10.1016/j.quascirev.2007.01.019.

Bronk Ramsey, C., 2009. Bayesian analysis of radiocarbon dates. Radiocarbon 51, 337–360. https://doi.org/10.1017/S0033822200033865.

Brooks, S.J., 2006. Fossil midges (Diptera: Chironomidae) as palaeoclimatic indicators for the Eurasian region. Quat. Sci. Rev. 25, 1894–1910. https://doi.org/10.1016/j.quascirev.2005.03.021.

Brooks, S.J., Birks, H.J.B., 2001. Chironomid-inferred air temperatures from lateglacial and Holocene sites in north-west Europe: progress and problems. Quat. Sci. Rev. 20, 1723–1741. https://doi.org/10.1002/1099-1417(200012)15:8<759::AID-JQS590>3.0.CO;2-V.

Brooks, S.J., Langdon, P.G., Heiri, O., 2007. The identification and use of Palaearctic Chironomidae larvae in palaeoecology. In: QRA Technical Guide No. 10. Quaternary Research Association, London, p. 276.

Cao, Y.M., Zhang, E.L., Langdon, P.G., Liu, E.F., Shen, J., 2014. Chironomid-inferred environmental change over the past 1400 years in the shallow, eutrophic Taibai Lake (south-east China): separating impacts of climate and human activity. Holocene 24, 581–590. https://doi.org/10.1177/0959683614522308.

Choudhury, M.I., Urrutia-Cordero, P., Zhang, H., Ekvall, M.K., Medeiros, L.R., Hansson, L.A., 2019. Charophytes collapse beyond a critical warming and brownification threshold in shallow lake systems. Sci. Total Environ. 661, 148–154. https://doi.org/10.1016/j.scitotenv.2019.01.177.

Coope, G.R., 2007. Coleoptera from the 2003 excavations of the mammoth skeleton at Niederweningen, Switzerland. Quat. Int. 164–165, 130–138. https://doi.org/10.1016/j.quaint.2006.10.004.

Cooper, A., Turney, C.S.M., Palmer, J., et al., 2021. A global environmental crisis 42,000 years ago. Science 371, 811–818. https://doi.org/10.1126/science.abb8677.

Cumming, B.F., Laird, K.R., Fritz, S.C., Verschuren, D., 2012. Tracking Holocene climatic change with aquatic biota preserved in lake sediments: case studies of commonly used numerical techniques. In: Birks, H.J.B., Lotter, A.F., Juggins, S., Smol, J.P. (Eds.), Tracking Environmental Changes in Lake Sediments, 5. Springer, Dordrecht, pp. 615–642. https://doi.org/10.1007/978-94-007-2745-8_20. Data Handling and Numerical Techniques.

Dansgaard, W., Johnsen, S.J., Clausen, H.B., Dahl-Jensen, D., Gundestrup, N.S., Hammer, C.U., Hvidberg, C.S., Steffensen, J.P., Sveinbj€ornsdottir, A.E., Jouzel, J., Bond, G., 1993. Evidence for general instability of past climate from a 250-kyr ice-core record. Nature 364, 218–220. https://doi.org/10.1038/364218a0.

Dean, W.E., 1999. The carbon cycle and biogeochemical dynamics in lake sediments. J. Paleolimnol. 21, 375–393. https://doi.org/10.1023/A:1008066118210.
den Heyer, C., Kalff, J., 1998. Organic matter mineralization rates in sediments: a within- and among-lake study. Limnol. Oceanogr. 43, 695–705. https://doi.org/10.4319/lo.1998.43.4.0695.
Denton, G.H., Alley, R.B., Comer, G.C., Broecker, W.S., 2005. The role of seasonality in abrupt climate change. Quat. Sci. Rev. 24, 1159–1182. https://doi.org/10.1016/j.quascirev.2004.12.002.
Eggermont, H., Heiri, O., 2012. The chironomid-temperature relationship: expression in nature and palaeoenvironmental implications. Biol. Rev. 87, 430–456. https://doi.org/10.1111/j.1469-185X.2011.00206.x.
Engels, S., Bohncke, S.J.P., Bos, J.A.A., Brooks, S.J., Heiri, O., Helmens, K.F., 2008a. Chironomid-based palaeotemperature estimates for northeast Finland during oxygen isotope stage 3. J. Paleolimnol. 40, 49–61. https://doi.org/10.1007/s10933-007-9133-y.
Engels, S., Bohncke, S.J.P., Bos, J.A.A., Heiri, O., Vandenberghe, J., Wallinga, J., 2008b. Environmental inferences and chironomid-based temperature reconstructions from fragmentary records of the Weichselian Early Glacial and Pleniglacial of the Niederlausitz area (eastern Germany). Palaeogeogr. Palaeoclimatol. Palaeoecol. 260, 405–416. https://doi.org/10.1016/j.palaeo.2007.12.005.
Engels, S., Bohncke, S.J.P., Heiri, O., Schaber, K., Sirocko, F., 2008c. The lacustrine sediment record of Oberwinkler Maar (Eifel, Germany): chironomid-based inferences of environmental changes during Oxygen Isotope Stage-3. Boreas 37, 414–425. https://doi.org/10.1111/j.1502-3885.2008.00033.x.
Engels, S., Self, A.E., Luoto, T.P., Brooks, S.J., Helmens, K.F., 2014. A comparison of three Eurasian chironomide–climate calibration datasets on a W–E continentality gradient and the implications for quantitative temperature reconstructions. J. Paleolimnol. 51, 529–547. https://doi.org/10.1007/s10933-014-9772-8.
Ferrington, L.C., 2008. Global diversity of non-biting midges (Chironomidae; Insecta-Diptera) in freshwater. Hydrobiologia 595, 447–455. https://doi.org/10.1007/s10750-007-9130-1.
Fuhrmann, F., Diensberg, B., Gong, X., Lohmann, G., Sirocko, F., 2020. Aridity synthesis for 8 selected key regions of the global climate system during the last 60 000 years. Clim. Past 16, 2221–2238. https://doi.org/10.5194/cp-16-2221-2020.
Furrer, H., Graf, H.R., Mäder, A., 2007. The mammoth site of Niederweningen, Switzerland. Quat. Int. 164–165, 85–97. https://doi.org/10.1016/j.quaint.2006.10.012.
Gandouin, E., Rioual, P., Pailles, C., Brooks, S.J., Ponel, P., Guiter, F., Djamali, M., Andrieu-Ponel, V., Birks, H.J.B., Leydet, M., Belkacem, D., Haas, J.N., Van der Putten, N., de Beaulieu, J.L., 2016. Environmental and climate reconstruction of the late-glacial-Holocene transition from a lake sediment sequence in Aubrac, French Massif Central: chironomid and diatom evidence. Palaeogeogr. Palaeoclimatol. Palaeoecol. 461, 292–309. https://doi.org/10.1016/j.palaeo.2016.08.039.
Haas, J.N., 1994. First identification key for charophyte oospores from central Europe. Eur. J. Phycol. 29, 227–235. https://doi.org/10.1080/09670269400650681.
Hajdas, I., Bonani, G., Furrer, H., Mäder, A., Schoch, W., 2007. Radiocarbon chronology of the mammoth site at Niederweningen, Switzerland: results from dating bones, teeth, wood, and peat. Quat. Int. 164–165, 98–105. https://doi.org/10.1016/j.quaint.2006.10.007.
Hajdas, I., Michczyński, A., Bonani, G., Wacker, L., Furrer, H., 2009. Dating bones near the limit of the radiocarbon dating method: study case mammoth from Niederweningen, ZH Switzerland. Radiocarbon 51, 675–680. https://doi.org/10.1017/S0033822200056010.
Hammarlund, D., 1994. Thesis. Stable Carbon and Oxygen Isotope Studies of Late Weichselian Lake Sediments in Southern Sweden and Northern Poland, with Palaeoclimatic Implications, 31. Department of Quaternary Geology, Lund University, p. 30.
Hammarlund, D., Edwards, T.W.D., Björck, S., Buchardt, B., Wohlfarth, B., 1999. Climate and environment during the Younger Dryas (GS-1) as reflected by composite stable isotope records of lacustrine carbonates at Torreberga, southern Sweden. J. Quat. Sci. 14, 17–28 https://doi.org/10.1002/(SICI)1099-1417(199902)14:1<17::AID-JQS406>3.0.CO;2-E.
Hammarlund, D., Björck, S., Buchardt, B., Israelson, C., Thomsen, C., 2003. Rapid hydrological changes during the Holocene revealed by stable isotope records of lacustrine carbonates from Lake Igelsjön, southern Sweden. Quat. Sci. Rev. 22, 353–370. https://doi.org/10.1016/S0277-3791(02)00091-4.
Heiri, O., Lotter, A.F., 2001. Effect of low counts sums on quantitative environmental reconstructions: an example using subfossil chironomids. J. Paleolimnol. 26, 343–350. https://doi.org/10.1023/A:1017568913302.
Heiri, O., Millet, L., 2005. Reconstruction of late glacial summer temperatures from chironomid assemblages in lac Lautrey (France). J. Quat. Sci. 20, 33–44. https://doi.org/10.1002/jqs.895.
Heiri, O., Lotter, A.F., 2008. Chironomidae (Diptera) in Alpine lakes: a study based on subfossil assemblages in lake surface sediments. Boletim do Museu Munic do Funchal Suppl 13, 177–184.
Heiri, O., Lotter, A.F., 2010. How does taxonomic resolution affect chironomid-based temperature reconstruction? J. Paleolimnol. 44, 589–601. https://doi.org/10.1007/s10933-010-9439-z.
Heiri, O., Lotter, A.F., Lemcke, G., 2001. Loss on ignition as a method for estimating organic and carbonate content in sediments: reproducibility and comparability of results. J. Paleolimnol. 25, 101–110. https://doi.org/10.1023/A:1008119611481.
Heiri, O., Brooks, S., Birks, H.J.B., Lotter, A.F., 2011. A 274-lake calibration data-set and inference model for chironomid-based summer air temperature reconstruction in Europe. Quat. Sci. Rev. 30, 3445–3456. https://doi.org/10.1016/j.quascirev.2011.09.006.
Heiri, O., Koinig, K.A., Spötl, C., Barrett, S., Brauer, A., Drescher-Schneider, R., Gaar, D., Ivy-Ochs, S., Kerschner, H., Luetscher, M., Moran, A., Nicolussi, K., Preusser, F., Schmidt, R., Schoeneich, P., Schwörer, C., Sprafke, T., Terhorst, B., Tinner, W., 2014. Palaeoclimate records 60–8 ka in the Austrian and Swiss Alps and their forelands. Quat. Sci. Rev. 106, 186–205. https://doi.org/10.1016/j.quascirev.2014.05.021.
Helmens, K.F., 2014. The Last Interglacial–Glacial cycle (MIS 5–2) re-examined based on long proxy records from central and northern Europe. Quat. Sci. Rev. 86, 115–143. https://doi.org/10.1016/j.quascirev.2013.12.012.
Helmens, K.F., Engels, S., 2010. Ice-free conditions in eastern Fennoscandia during early Marine Isotope Stage 3: lacustrine records. Boreas 39, 399–409. https://doi.org/10.1111/j.1502-3885.2010.00142.x.
Helmens, K.F., Bos, J.A.A., Engels, S., Van Meerbeeck, C.J., Bohncke, S.J.P., Renssen, H., Heiri, O., Brooks, S.J., Seppä, H., Birks, H.J.B., Wohlfarth, B., 2007. Present-day temperatures in northern scandinavian during the last glaciation. Geology 35, 987–990. https://doi.org/10.1130/G23995A.1.
Helmens, K.F., Katrantsiotis, C., Salonen, J.S., Shala, S., Bos, J.A.A., Engels, S., Kuosmanen, N., Luoto, T.P., Väliranta, M., Luoto, M., Ojala, A., Risberg, J., Weckström, J., 2018. Warm summers and rich biotic communities during N-Hemisphere deglaciation. Global Planet. Change 167, 61–73. https://doi.org/10.1016/j.gloplacha.2018.05.004.
Holzkämper, S., Spötl, C., Mangini, A., 2005. High-precision constraints on timing of Alpine warm periods during the middle to late Pleistocene using speleothem growth periods. Earth Planet Sci. Lett. 236, 751–764. https://doi.org/10.1016/j.epsl.2005.06.002.
Horton, T.W., Defliese, W.F., Tripati, A.K., Oze, C., 2016. Evaporation induced $^{18}O$ and $^{13}C$ enrichment in lake systems: a global perspective on hydrologic balance effects. Quat. Sci. Rev. 131, 365–379. https://doi.org/10.1016/j.quascirev.2015.06.030.
Ilyashuk, E.A., Ilyashuk, B.P., Hammarlund, D., Larocque, I., 2005. Holocene climatic and environmental changes inferred from midge records (Diptera: Chironomidae, Chaoboridae, Ceratopogonidae) at Lake Berkut, southern Kola Peninsula, Russia. Holocene 15, 897–914. https://doi.org/10.1191/0959683605hl865ra.
Ilyashuk, E.A., Ilyashuk, B.P., Kolka, V.V., Hammarlund, D., 2013. Holocene climate variability on the Kola Peninsula, Russian Subarctic, based on aquatic invertebrate records from lake sediments. Quat. Res. 79, 350–361. https://doi.org/10.1016/j.yqres.2013.03.005.
Ilyashuk, E.A., Ilyashuk, B.P., Heiri, O., Spötl, C., 2020. Summer temperatures and lake development during the MIS 5a interstadial: new data from the Unterangerberg palaeolake in the Eastern Alps, Austria. Palaeogeogr. Palaeoclimatol. Palaeoecol. 560, 110020. https://doi.org/10.1016/j.palaeo.2020.110020.
ISO 10694, 1995. Soil Quality – Determination of Organic and Total Carbon with Dry Combustion Method ("elemental Analysis").
ISO 13878, 1998. Soil Quality – Determination of Total Nitrogen with Dry Combustion Method ("elemental Analysis").
Ito, E., 2001. Application of stable isotope techniques to inorganic and biogenic carbonates. In: Last, W.M., Smol, J.P. (Eds.), Tracking Environmental Change Using Lake Sediments, 2. Kluwer, Dordrecht, pp. 351–371. Physical and Geochemical Methods.
Janecek, B., Moog, O., Moritz, C., Saxl, R., 2002. Diptera: Chironomidae: Orthocladiinae. Teil III. In: Moog, O. (Ed.), Fauna Aquatica Austriaca, second ed. Wasserwirtschaftskataster, Bundesministerium für Land- und Forstwirtschaft, Umwelt und Wasserwirtschaft, Wien.
Jones, R.T., Marshall, J.D., Crowley, S.F., Bedford, A., Richardson, N., Bloemendal, J., Oldfield, F., 2002. A high resolution, multiproxy Late-glacial record of climate change and intrasystem responses in northwest England. J. Quat. Sci. 17, 329–340. https://doi.org/10.1002/jqs.683.
Jonsson, C.E., Andersson, S., Rosqvist, G.C., Leng, M.J., 2010. Reconstructing past atmospheric circulation changes using oxygen isotopes in lake sediments from Sweden. Clim. Past 6, 49–62. https://doi.org/10.5194/cp-6-49-2010.
Jost-Stauffer, M.A., Coope, G.R., Schlüchter, C., 2005. Environmental and climatic reconstructions during marine oxygen isotope stage 3 from Gossau, Swiss Midlands, based on coleopteran assemblages. Boreas 34, 53–60. https://doi.org/10.1111/j.1502-3885.2005.tb01004.x.
Juggins, S., Birks, J., 2012. Quantitative environmental reconstructions from biological data. In: Birks, H.J.B., Lotter, A.F., Juggins, S., Smol, J.P. (Eds.), Tracking Environmental Change Using Lake Sediments, 5. Springer, Dordrecht, pp. 431–494. https://doi.org/10.1007/978-94-007-2745-8_14. Data Handling and Numerical Techniques.
Landolt, E., 1992. Unsere Alpenflora. Brugg. Verl. Schweiz. Alpen-Club, p. 318.
Langdon, P.G., Ruiz, Z., Wynne, S., Sayer, C.D., Davidson, T.A., 2010. Ecological influences on larval chironomid communities in shallow lakes: implications for palaeolimnological interpretations. Freshw. Biol. 55, 531–545. https://doi.org/10.1111/j.1365-2427.2009.02345.x.
Larocque, I., Hall, R.I., Grahn, E., 2001. Chironomids as indicators of climate change: a 100-lake training set from a subarctic region of northern Sweden (Lapland). J. Paleolimnol. 26, 307–322. https://doi.org/10.1023/A:1017524101783.
Larocque-Tobler, I., Heiri, O., Wehrli, M., 2010. Lateglacial and Holocene temperature changes at Egelsee, Switzerland, reconstructed using subfossil chironomids. J. Paleolimnol. 43, 649–666. https://doi.org/10.1007/s10933-009-9358-z.
Leng, M.J., Henderson, A.C.G., 2013. Recent advances in isotopes as palaeolimnological proxies. J. Paleolimnol. 49, 481–496. https://doi.org/10.1007/s10933-012-9667-5.
Leng, M.J., Marshall, J.D., 2004. Palaeoclimate interpretation of stable isotope data from lake sediment archives. Quat. Sci. Rev. 23, 811–831. https://doi.org/10.1016/j.quascirev.2003.06.012.
Li, C., Born, A., 2019. Coupled atmosphere-ice-ocean dynamics in Dansgaard-Oeschger events. Quat. Sci. Rev. 203, 1–20. https://doi.org/10.1016/j.quascirev.2018.10.031.

Lisiecki, L.E., Raymo, M.E., 2005. A Pliocenee-Pleistocene stack of 57 globally distributed benthic $\delta^{18}O$ records. Paleoceanography 20, PA1003. https://doi.org/10.1029/2004PA001071.

Lotter, A.F., Birks, H.J.B., Hofmann, W., Marchetto, A., 1997. Modern diatom, cladocera, chironomid, and chrysophyte cyst assemblages as quantitative indicators for the reconstruction of past environmental conditions in the Alps. I. Climate. J. Paleolimnol. 18, 395–420. https://doi.org/10.1023/A:1007982008956.

Lotter, A.F., Walker, I.R., Brooks, S.J., Hofmann, W., 1999. An intercontinental comparison of chironomid palaeotemperature inference models: Europe vs North America. Quat. Sci. Rev. 18, 717–735. https://doi.org/10.1016/S0277-3791(98)00044-4.

Luoto, T.P., 2009. Subfossil Chironomidae (Insecta: Diptera) along a latitudinal gradient in Finland: development of a new temperature inference model. J. Quat. Sci. 24, 150–158. https://doi.org/10.1002/jqs.1191.

Makarchenko, E.A., 1985. Chironomids of the far east of USSR. In: The Subfamilies Podonominae, Diamesinae, and Prodiamesinae (Diptera, Chironomidae). DVNC AN SSSR, Vladivostok.

Mayr, C., Brandlmeier, B., Diersche, V., Stojakowits, P., Kirscher, U., Matzke-Karasz, R., Bachtadse, V., Eigler, M., Haas, U., Lempe, B., Reimer, P.J., Spötl, C., 2017. Nesseltalgraben, a new reference section of the last glacial period in southern Germany. J. Paleolimnol. 58, 213–229. https://doi.org/10.1007/s10933-017-9972-0.

Mayr, C., Stojakowits, P., Lempe, B., Blaauw, M., Diersche, V., Grohganz, M., López Correa, M., Ohlendorf, C., Reimer, P., Zolitschka, B., 2019. High-resolution geochemical record of environmental changes during MIS 3 from the northern Alps (Nesseltalgraben, Germany). Quat. Sci. Rev. 218, 122–136. https://doi.org/10.1016/j.quascirev.2019.06.013.

Medeiros, A.S., Quinlan, R., 2011. The distribution of the Chironomidae (Insecta: Diptera) along multiple environmental gradients in lakes and ponds of the eastern Canadian Arctic. Can. J. Fish. Aquat. Sci. 68, 1511–1527. https://doi.org/10.1139/f2011-076.

Meyers, P.A., Teranes, J.L., 2001. Sediment organic matter. In: Last, W.M., Smol, J.P. (Eds.), Tracking Environmental Changes Using Lake Sediment, 2. Kluwer Academic, Dordrecht, pp. 239–270. https://doi.org/10.1007/0-306-47670-3_9. Physical and Geochemical Methods.

Moller Pillot, H.K.M., 2008. Identification and ecology of the genus *Smittia* Holmgren in the Netherlands (Diptera: Chironomidae). Tijdschr. Entomol. 151, 245–270.

Moseley, G.E., Spötl, C., Svensson, A., Cheng, H., Brandstätter, S., Edwards, R.L., 2014. Multi-speleothem record reveals tightly coupled climate between central Europe and Greenland during Marine Isotope Stage 3. Geology 42, 1043–1046. https://doi.org/10.1130/G36063.1.

Mothes, G., 1968. Einige ökologisch interessante Chironomiden aus dem Stechlinseegebiet. Ann. Zool. Fenn. 5, 92–96.

North Greenland Ice Core Project Members, 2004. High-resolution record of Northern Hemisphere climate extending into the last interglacial period. Nature 431, 147–151. https://doi.org/10.1038/nature02805.

Ortner, H., Stingl, H., 2001. Facies and basin development of the Oligocene in the lower Inn Valley, Tyrol/Bavaria. In: Piller, W., Rasser, M.W. (Eds.), Paleogene of the Eastern Alps, Schriftenreihe der Erdwissenschaftlichen Kommission der Österreichischen Akademie der Wissenschaften, 14, pp. 153–196.

Pełechaty, M., Pukacz, A., Apolinarska, K., Pełechata, A., Siepak, M., 2013. The significance of *Chara* vegetation in the precipitation of lacustrine calcium carbonate. Sedimentology 60, 1017–1035. https://doi.org/10.1111/sed.12020.

Polášková, V., Schenková, J., Bílková, M., Poláková, M., Šorfová, V., Polášek, M., Schlaghamerský, J., Horsák, M., 2020. Drivers of small-scale Diptera distribution in aquatic-terrestrial transition zones of spring fens. Wetlands 40, 235–247. https://doi.org/10.1007/s13157-019-01171-w.

Porinchu, D.F., Cwynar, L.C., 2000. The distribution of freshwater Chironomidae (Insecto: Diptera) across Treeline near the lower Lena river, Northeast Siberia, Russia. Arctic Antarct. Alpine Res. 32, 429–437. https://doi.org/10.1080/15230430.2000.12003387.

Porinchu, D.F., Rolland, N., Moser, K., 2009. Development of a chironomid-based air temperature inference model for the central Canadian Arctic. J. Paleolimnol. 41, 349–368. https://doi.org/10.1007/s10933-008-9233-3.

Preusser, F., 2004. Towards a chronology of the late Pleistocene in the northern alpine foreland. Boreas 33, 95–210. https://doi.org/10.1111/j.1502-3885.2004.tb01141.x.

Quinlan, R., Smol, J.P., Hall, R.I., 1998. Quantitative inferences of past hypolimnetic anoxia in south-central Ontario lakes using fossil midges (Diptera: Chironomidae). Can. J. Fish. Aquat. Sci. 55, 587–596. https://doi.org/10.1139/f97-279.

Rasmussen, S.O., Bigler, M., Blockley, S.P., Blunier, T., Buchardt, S.L., Clausen, H.B., Cvijanovic, I., Dahl-Jensen, D., Johnsen, S.J., Fischer, H., Gkinis, V., Guillevic, M., Hoek, W.Z., Lowe, J.J., Pedro, J.B., Popp, T., Seierstad, I.K., Steffensen, J.P., Svensson, A.M., Vallelonga, P., Vinther, B.M., Walker, M.J.C., Wheatley, J.J., Winstrup, M., 2014. A stratigraphic framework for abrupt climatic changes during the Last Glacial period based on three synchronized Greenland ice-core records: refining and extending the INTIMATE event stratigraphy. Quat. Sci. Rev. 106, 14–28. https://doi.org/10.1016/j.quascirev.2014.09.007.

Rees, A.B.H., Cwynar, L.C., Cranston, P.S., 2008. Midges (Chironomidae, Ceratopogonidae, Chaoboridae) as a temperature proxy: a training set from Tasmania, Australia. J. Paleolimnol. 40, 1159–1178. https://doi.org/10.1007/s10933-008-9222-6.

Reimer, P., Austin, W.E.N., Bard, E., Bayliss, A., Blackwell, P.G., Bronk Ramsey, C., Butzin, M., Cheng, H., Edwards, R.L., Friedrich, M., Grootes, P.M., Guilderson, T.P., Hajdas, I., Heaton, T.J., Hogg, A.G., 2020. The IntCal20 Northern Hemisphere radiocarbon age calibration curve (0-55 kcal BP). Radiocarbon 62, 725–757. https://doi.org/10.1017/RDC.2020.41.

Scheffer, M., 1990. Multiplicity of stable states in freshwater systems. Hydrobiologia 200, 475–486. https://doi.org/10.1007/BF02530365.

Seguinot, J., Ivy-Ochs, S., Jouvet, G., Huss, M., Funk, M., Preusser, F., 2018. Modelling last glacial cycle ice dynamics in the Alps. Cryosphere 12, 3265–3285. https://doi.org/10.5194/tc-12-3265-2018.

Self, A.E., Brooks, S.J., Birks, H.J.B., Nazarova, L., Porinchu, D., Odland, A., Yang, H., Jones, V.J., 2011. The distribution and abundance of chironomids in high-latitude Eurasian lakes with respect to temperature and continentality: development and application of new chironomid-based climate-inference models in northern Russia. Quat. Sci. Rev. 30, 1122–1141. https://doi.org/10.1016/j.quascirev.2011.01.022.

Shackleton, N.J., Hall, M.A., Vincent, E., 2000. Phase relationships between millennial-scale events 64,000–24,000 years ago. Paleoceanography 15, 565–569. https://doi.org/10.1029/2000PA000513.

Siddall, M., Rohling, E.J., Almogi-Labin, A., Hemleben, C., Meischner, D., Schmelzer, I., Smeed, D.A., 2003. Sea-level fluctuations during the last glacial cycle. Nature 423, 853–858. https://doi.org/10.1038/nature01690.

Siddall, M., Rohling, E.J., Thompson, W.G., Waelbroeck, C., 2008. Marine isotope stage 3 sea level fluctuations: data synthesis and new outlook. Rev. Geophys. 46, 109–129. https://doi.org/10.1029/2007RG000226.

Smith, D.G., 1991. Lacustrine deltas. Can. Geogr. 35, 311–316. https://doi.org/10.1111/j.1541-0064.1991.tb01106.x.

Spötl, C., Mangini, A., 2002. Stalagmite from the Austrian Alps reveals Dansgaard–Oeschger events during isotope stage 3: implications for the absolute chronology of Greenland ice cores. Earth Planet Sci. Lett. 203, 507–518. https://doi.org/10.1016/S0012-821X(02)00837-3.

Spötl, C., Mangini, A., 2007. Speleothems and paleoglaciers. Earth Planet Sci. Lett. 254, 323–331. https://doi.org/10.1016/j.epsl.2006.11.041.

Spötl, C., Vennemann, T.W., 2003. Continuous-flow isotope ratio mass spectrometric analysis of carbonate minerals. Rapid Commun. Mass Spectrom. 17, 1004–1006. https://doi.org/10.1002/rcm.1010.

Spötl, C., Mangini, A., Richards, D.A., 2006. Chronology and paleoenvironment of marine isotope stage 3 from two high-elevation speleothems, Austrian Alps. Quat. Sci. Rev. 25, 1127–1136. https://doi.org/10.1016/j.quascirev.2005.10.006.

Spötl, C., Reimer, P.J., Göhlich, U.B., 2018. Mammoths inside the Alps during the last glacial period: radiocarbon constraints from Austria and palaeoenvironmental implications. Quat. Sci. Rev. 190, 11–19. https://doi.org/10.1016/j.quascirev.2018.04.020.

Starnberger, R., Drescher-Schneider, R., Reitner, J.M., Rodnight, H., Reimer, P.J., Spötl, C., 2013a. Late Pleistocene climate change and landscape dynamics in the Eastern Alps: The inner-alpine Unterangerberg record (Austria). Quat. Sci. Rev. 68, 17–62. https://doi.org/10.1016/j.quascirev.2013.02.008.

Starnberger, R., Rodnight, H., Spötl, C., 2013b. Luminescence dating of fine-grain lacustrine sediments from the Late Pleistocene Unterangerberg site (Tyrol, Austria). Aust. J. Earth Sci. 106, 4–15.

Stojakowits, P., Mayr, C., Lücke, A., Wissel, H., Hedenäs, L., Lempe, B., Friedmann, A., Diersche, V., 2020. Impact of climatic extremes on Alpine ecosystems during MIS 3. Quat. Sci. Rev. 239, 106333. https://doi.org/10.1016/j.quascirev.2020.106333.

Talbot, M.R., 1990. A review of the palaeohydrological interpretation of carbon and oxygen isotopic ratios in primary lacustrine carbonates. Chem. Geol. Isot. Geosci. 80, 261–279. https://doi.org/10.1016/0168-9622(90)90009-2.

ter Braak, C.J.F., Juggins, S., 1993. Weighted averaging partial least squares regression (WA-PLS): an improved method for reconstructing environmental variables from species assemblages. Hydrobiologia 269/270, 485–502. https://doi.org/10.1007/bf00028046.

Thompson, H.A., White, J.R., Pratt, L.M., 2018. Spatial variation in stable isotopic composition of organic matter of macrophytes and sediments from a small Arctic lake in west Greenland. Arctic Antarct. Alpine Res. 50, e1420282 https://doi.org/10.1080/15230430.2017.1420282.

Tockner, K., Stanford, J.A., 2002. Riverine flood plains: present state and future trends. Environ. Conserv. 29, 308–330. https://doi.org/10.1017/S037689290200022X.

Tütken, T., Furrer, H., Vennemann, T.W., 2007. Stable isotope compositionsof mammoth teeth from Niederweningen, Switzerland: implications for the Late Pleistocene climate, environment, and diet. Quat. Int. 164–165, 139–150. https://doi.org/10.1016/j.quaint.2006.09.004.

Van de Weyer, K., Schmidt, C., 2018a. Bestimmungsschlüssel für die aquatischen Makrophyten (Gefäßpflanzen, Armleuchteralgen und Moose) in Deutschland: Band 1: Bestimmungsschlüssel. Fachbeiträge des LfU Brandenburg 119, 180. Landesamt für Umwelt Brandenburg, Potsdam.

Van de Weyer, K., Schmidt, C., 2018b. Bestimmungsschlüssel für die aquatischen Makrophyten (Gefäßpflanzen, Armleuchteralgen und Moose) in Deutschland: Band 2: Abbildungen. 2., überarbeitete Auflage. Fachbeiträge des LfU Brandenburg 120, 394. Landesamt für Umwelt Brandenburg, Potsdam.

Van Meerbeeck, C.J., Renssen, H., Roche, D.M., 2009. How did marine isotope stage 3 and last glacial maximum climates differ? – perspectives from equilibrium simulations. Clim. Past 5, 33–51. https://doi.org/10.5194/cp-5-33-2009.

Van Meerbeeck, C.J., Renssen, H., Roche, D.M., Wohlfarth, B., Bohncke, S.J.P., Bos, J.A.A., Engels, S., Helmens, K.F., Sánchez-Goñi, M.F., Svensson, A., Vandenberghe, J., 2011. The nature of MIS 3 stadialeinterstadial transitions in Europe: new insights from modeledata comparisons. Quat. Sci. Rev. 30, 3618–3637. https://doi.org/10.1016/j.quascirev.2011.08.002.

Vogel, H., Wagner, B., Zanchetta, G., Sulpizio, R., Rosén, P., 2010. A paleoclimate record with tephrochronological age control for the last glacial–interglacial cycle from Lake Ohrid, Albania and Macedonia. J. Paleolimnol. 44, 295–310. https://doi.org/10.1002/jqs.1311.

Walker, I.R., 1995. Chironomids as indicators of past environmental change. In: Armitage, P.D., Cranston, P.S., Pinder, L.C.V. (Eds.), The Chironomidae. The Biology and Ecology of Non-biting Midges. Chapman and Hall, London, pp. 405–422.
Walker, I.R., 2013. Chironomid overview. In: Elias, S.A., Mock, C.J. (Eds.), Encyclopedia of Quaternary Sciences, second ed. Elsevier, London, pp. 355–360.
Wiik, E., Bennion, H., Sayer, C.D., Willby, N.J., 2013. Chemical and biological responses of marl lakes to eutrophication. Freshw. Rev. 6, 35–62. https://doi.org/10.1608/FRJ-6.2.630.
Wolff, E.W., Chappellaz, J., Blunier, T., Rasmussen, S.O., Svensson, A., 2010. Millennial-scale variability during the last glacial: the ice core record. Quat. Sci. Rev. 29, 2828–2838. https://doi.org/10.1016/j.quascirev.2009.10.013.